

The Developmental Testbed Center's Final Report on the Inter-Comparison of the WRFv3.3.1 AFWA Operational and RRTMG-Replacement Configurations

Point of Contact: Michelle Harrold
20 January 2012

Executive Summary

The Weather Research and Forecasting (WRF) model is a mesoscale numerical weather prediction system utilized in both research and operational forecasting applications. The model is configurable to the users' requirements and suitable for a broad spectrum of weather regimes. Due to the flexibility offered by the model, it is necessary to rigorously test select configurations and evaluate the performance for specific applications. To assess the performance of the updated Rapid Radiative Transfer Model (RRTMG) long- and short-wave radiation schemes, which have been available since WRF v3.1, the Developmental Testbed Center (DTC) performed testing and evaluation with the Advanced Research WRF (ARW) dynamic core for two physics suite configurations at the request of the sponsor, the Air Force Weather Agency (AFWA). One configuration was based on AFWA's Operational Configuration, which is a baseline for testing and evaluating new options available in the WRF system. The second configuration substituted AFWA's current operational long- and short-wave radiation schemes (RRTM/Dudhia) with the RRTMG radiation schemes. This report focuses on the pair-wise differences between the standard verification metrics for the two configurations, including an assessment of the statistical significance (SS) and practical significance (PS). Bias-corrected root-mean-square-error (BCRMSE) and bias were evaluated for surface and upper air temperature, dew point temperature, and wind speed; Gilbert Skill Score (GSS) and frequency bias were evaluated for 3-hourly and daily quantitative precipitation forecasts (QPF). The following points summarize the SS and PS differences seen in the verification results between the AFWA and RRTMG configurations.

- Upper air temperature
 - BCRMSE: the RRTMG configuration was SS favored at most levels below 300 hPa for most lead times and temporal aggregations; no PS differences were observed
 - Bias: for all temporal aggregations, persistent PS pair-wise differences favoring the RRTMG configuration at and below 700 hPa were noted
- Upper air dew point temperature
 - BCRMSE: all SS/PS pair-wise differences favor the RRTMG configuration, which most frequently occur at 850 hPa and occasionally at additional levels
 - Bias: with exception to several forecast lead times during the summer aggregation that favor the RRTMG configuration, all other PS pair-wise differences favor the AFWA configuration
- Upper air wind speed
 - BCRMSE: SS pair-wise differences overwhelmingly favor the RRTMG configuration; however, none are PS
 - Bias: pair-wise differences generally favor the AFWA configuration; however, none are PS
- Surface temperature
 - BCRMSE: a number of SS pair-wise differences are present but the favored configuration depends on the temporal aggregation and lead time; PS pair-wise

- differences that are seen occur in the fall and winter aggregations and favor the RRTMG configuration
- Bias: SS/PS pair-wise differences predominantly indicate the RRTMG configuration is a better performer, with a consistent exception during the winter aggregation for forecast lead times valid between 06 – 09 UTC, which favor the AFWA configuration
 - Surface dew point temperature
 - BCRMSE: a diurnal trend in which configuration is favored is noted, with the AFWA configuration typically performing better during times valid in the afternoon/early evening hour and the RRTMG configuration generally favored during times valid overnight/early morning; however, only one difference is PS
 - Bias: the RRTMG configuration is generally favored during times valid overnight/early morning during the summer and fall aggregations; for all other seasonal aggregations and lead times, many PS differences are noted and favor the AFWA configuration
 - Surface wind speed
 - BCRMSE: for both initializations and all temporal aggregations, many SS pair-wise differences are seen, with nearly all favoring the RRTMG configuration; however, none are PS
 - Bias: for both initializations and all temporal aggregations, many SS pair-wise differences are seen, with nearly all favoring the AFWA configuration; however, none are PS
 - Three-hourly QPF
 - GSS: the AFWA configuration is generally a better performer, with differences occurring at an assortment of thresholds and lead times; however, during the winter season the majority of differences favor the RRTMG configuration, namely at the lowest thresholds
 - Frequency Bias: no SS pair-wise differences noted
 - Daily QPF
 - GSS: SS pair-wise differences favor the RRTMG configuration at the 0.01" threshold for a majority of temporal aggregations and lead times for both initializations; all differences at higher thresholds favor the AFWA configuration
 - Frequency Bias: no SS pair-wise differences noted
 - Regardless of initialization or temporal aggregation, the GO Index indicates the RRTMG configuration is more skillful than the AFWA configuration.

1. Introduction

The Weather Research and Forecasting (WRF) model is a mesoscale numerical weather prediction system utilized in both research and operational forecasting applications. The model is configurable to the users' requirements and suitable for a broad spectrum of weather regimes. Due to the flexibility offered by the model, it is necessary to rigorously test select configurations and evaluate the performance for specific applications. The Air Force Weather Agency (AFWA) is interested in improvements to their operational configuration. The Developmental Testbed Center (DTC) performed testing and evaluation with the Advanced Research WRF (ARW) dynamic core (Skamarock et al. 2008) for two physics suite configurations at the request of the sponsor, AFWA. One configuration was based on AFWA's Operational Configuration (OC), which provides a baseline for testing and evaluating new options available in the WRF system. The second configuration substituted AFWA's current operational long- and short-wave radiation schemes [Rapid Radiative Transfer Model (RRTM)/Dudhia] with the updated Rapid Radiative Transfer Model (RRTMG) radiation schemes (Iacono et al. 2008), which have been available since WRF v3.1. To assess the performance of these schemes, verification statistics were computed for the two configurations, and the analysis was based on the objective statistics of the model output. A brief analysis of computational resources required to run each configuration is also included. In addition to documenting the performance of the two configurations against each

other, both of these configurations will be designated as DTC Reference Configurations (RCs) and the results made available to the WRF community.

2. Experiment Design

For this test, the end-to-end forecast system consisted of the WRF Preprocessing System (WPS), WRF, Unified Postprocessor (UPP) and the NCAR Command Language (NCL) for graphics generation. Post-processed forecasts were verified using the Model Evaluation Tools (MET). In addition, the full data set was archived and made available for dissemination to the user community. The codes utilized were based on the official released versions of WPS (v3.3.1), WRF (v3.3.1), UPP (v1.0), and MET (v3.0.1). MET included relevant bug fixes that were checked into the code repository prior to testing.

2.1 Forecast Periods

Forecasts were initialized every 36 hours from 2 June 2008 through 31 May 2009, consequently creating a default of initialization times including both 00 and 12 UTC, for a total of 243 cases (see Appendix A for a list of the cases). The forecasts were run out to 48 hours with output files generated every 3 hours.

The tables below list the forecast initializations that failed to complete the end-to-end process; the missing data and reason for failure is described in the table. All missing forecasts were due to missing or bad input data sets, not model crashes. A total of 232 cases ran to completion and were used in the verification results.

Missing forecasts:

Affected Cycle	Missing data	Reason
2008071000	WRF output	Missing SST input data
2008091512	WRF output	Bad SST input data
2008101512	WRF output	Bad SST input data
2008101700	WRF output	Bad SST input data
2008101812	WRF output	Bad SST input data
2008102112	WRF output	Missing AGRMET input data
2008121112	WRF output	Bad SST input data
2009040112	WRF output	Bad SST input data
2009042212	WRF output	Bad SST input data
2008052400	WRF output	Missing SST input data
2008052512	WRF output	Missing SST input data

Missing verification:

Affected Cycle	Missing data	Reason
2008071300	Incomplete sfc/upper-air verification beyond 33 h	Missing Prepbufr data
2008071412	Incomplete sfc/upper-air verification for first 21 h	Missing Prepbufr data
2008101400	Incomplete sfc/upper-air verification beyond 39 h	Missing Prepbufr data
2008110100	Incomplete 3-h QPF verification beyond 21 h	Missing ST2 analysis
2008110212	Incomplete 3-h QPF verification for first 12 h	Missing ST2 analysis
2008012100	Incomplete sfc/upper-air verification for 18 – 21 h	Missing Prepbufr data
2009012700	Incomplete sfc/upper-air verification for 24 – 27 h	Missing Prepbufr data

2.2 Initial and Boundary Conditions

Initial conditions (ICs) and lateral boundary conditions (LBCs) were derived from the 0.5° x 0.5° Global Forecast System (GFS). Output from AFWA's Agricultural Meteorological Modeling

(AGRMET) System was used for the lower boundary conditions (LoBCs). In addition, a daily, real-time sea surface temperature product from Fleet Numerical Meteorology and Oceanography Center (FNMOC) was used to initialize the sea surface temperature (SST) field for the forecasts. The time-invariant components of the LoBCs (topography, soil, vegetation type, etc.) were derived from United States Geological Survey (USGS) input data. WPS was run once, and the same output data were used for initializing both configurations of the model.

2.3 Model Configuration Specifics

2.3.1 Domain Configuration

A 15-km contiguous U.S. (CONUS) grid was employed for this test. The domain (Fig. 1) was selected such that it covers complex terrain, plains, and coastal regions spanning from the Gulf of Mexico, north, to Central Canada in order to capture diverse regional effects for worldwide comparability. The domain was 403 x 302 gridpoints, for a total of 121,706 gridpoints. The Lambert-Conformal map projection was used and the model was configured to have 56 vertical levels (57 sigma entries) with the model top at 10 hPa.

2.3.2 Other Aspects of Model Configuration

The table below lists the two physics suite configurations that were used for each model configuration in this test. The model configuration based on AFWA's OC will be referred to as AFWA, while the companion configuration will be referred to as RRTMG.

	AFWA OC (AFWA)	RRTMG replacement (RRTMG)
Microphysics	WRF Single-Moment 5 scheme	WRF Single-Moment 5 scheme
Radiation LW and SW	RRTM/Dudhia schemes	RRTMG/RRTMG
Surface Layer	Monin-Obukhov similarity theory	Monin-Obukhov similarity theory
Land-Surface Model	Noah	Noah
Planetary Boundary Layer	Yonsei University scheme	Yonsei University scheme
Convection	Kain-Fritsch scheme	Kain-Fritsch scheme

Both configurations were run with a long timestep of 90 s, and an acoustic step of 4 was used. Calls to the boundary layer, and microphysics were performed every time step, whereas the cumulus parameterization was called every 5 minutes and every 30 minutes for the radiation.

The ARW solver offers a number of run-time options for the numerics, as well as various filter and damping options (Skamarock et al. 2008). The ARW was configured to use the following numeric options: 3rd-order Runge-Kutta time integration, 5th-order horizontal momentum and scalar advection, and 3rd-order vertical momentum and scalar advection. In addition, the following filter/damping options were utilized: three-dimensional divergence damping (coefficient 0.1), external mode filter (coefficient 0.01), off-center integration of vertical momentum and geopotential equations (coefficient 0.1), vertical-velocity damping, and a 5-km-deep diffusive damping layer at the top of the domain (coefficient 0.02). Positive-definite moisture advection was also turned on.

Appendix B provides relevant portions of the *namelist.input* file.

2.4 Post-processing

The *unipost* program within UPP was used to destagger the forecasts, to generate derived meteorological variables, including mean sea level pressure, and to vertically interpolate fields to isobaric levels. The post-processed files included two- and three-dimensional fields on constant pressure levels, both of which were required by the plotting and verification programs. Three-

dimensional post-processed fields on model native vertical coordinates were also output and used to generate graphical forecast sounding plots.

3. Computational Efficiency

For the 232 initializations that ran to completion, the central processing unit (CPU) time required to run WRF for the two configurations was calculated to assess the increase in computational demands when using the two different long- and short-wave radiation schemes. This testing effort was conducted on an IBM system, and each model initialization was run on 64 processors. The updated RRTMG schemes, being relatively more sophisticated than the RRTM/Dudhia schemes, were expected to increase the CPU time for the RRTMG configuration. Overall, a consistent difference in computational run time between the AFWA configuration and the RRTMG configuration was observed (Fig. 2) indicating the RRTMG configuration, on average, takes 26.9% longer to run to completion.

4. Model Verification

The MET package was used to generate objective model verification. MET is comprised of grid-to-point verification, which was utilized to compare gridded surface and upper-air model data to point observations, as well as grid-to-grid verification, which was utilized to verify QPF. Verification statistics generated by MET for each retrospective case were loaded into a MySQL database. Data was then retrieved from this database to compute and plot specified aggregated statistics using routines developed by the DTC in the statistical programming language, R.

Several domains were verified for the surface and upper air, as well as precipitation variables. Area-average results were computed for the full domain, as well as the 14 sub-domains shown in Fig. 3. Only the full domain is described in detail for this report; however, all sub-domain results are available on the DTC website (http://www.dtcenter.org/eval/afwa_test/wrf_v3.3.1/index.php). In addition to the regional stratification, the verification statistics were also stratified by vertical level and lead time for the 00 UTC and 12 UTC initialization hours combined, and by forecast lead time and precipitation threshold for 00 UTC and 12 UTC initialized forecasts individually for surface fields in order to preserve the diurnal signal.

Each type of verification metric is accompanied by confidence intervals (CIs), at the 99% level, computed using the appropriate statistical method. Both configurations were run for the same cases allowing for a pair-wise difference methodology to be applied, as appropriate. The CIs on the pair-wise differences between statistics for the two configurations objectively determines whether the differences are statistically significant (SS); if the CIs on the median pair-wise difference statistics include zero, the differences are not statistically significant. Due to the nonlinear attributes of frequency bias, it is not amenable to a pair-wise difference comparison. Therefore, the more powerful method to establish SS could not be used and, thus, a more conservative estimate of SS was employed based solely on whether the aggregate statistics, with the accompanying CIs, overlapped between the two configurations. If no overlap was noted for a particular threshold, the differences between the two configurations were considered SS.

Due to the large number of cases used in this test, many SS pair-wise differences were anticipated. In many cases, the magnitude of the SS differences was quite small and did not yield practically meaningful results. Therefore, in addition to determining SS, the concept of establishing practical significance (PS) was also implemented for this test. PS was determined by filtering results to highlight pair-wise differences greater than the operational measurement uncertainty requirements and instrument performance as specified by the World Meteorological Organization (WMO; http://www.wmo.int/pages/prog/www/IMOP/publications/CIMO-Guide/1st-Suppl-to-7th_draft/pdf/Annex_I_1B.pdf). To establish PS between the two configurations, the

following criteria was applied: temperature and dew point temperature differences greater than 0.1 K and wind speed differences greater than 0.5 m s⁻¹. PS was not considered for metrics used in precipitation verification [i.e., Gilbert Skill Score (GSS) or frequency bias] because those metrics are calculated via a contingency table, which is based on counts of yes and no forecasts.

4.1 Temperature, Dew Point Temperature, and Winds

Forecasts of surface and upper air temperature, dew point temperature, and wind were bilinearly interpolated to the location of the observations (METARs and RAOBS) within the National Centers for Environmental Prediction (NCEP) North American Data Assimilation System (NDAS) prepbuf files. Objective model verification statistics were then generated for surface (using METAR) and upper air (using RAOBS) temperature, dew point temperature, and wind. Because shelter-level variables are not available at the initial model time, surface verification results start at the 3-hour lead time and go out 48 hours by 3-hour increments. For upper air, verification statistics were computed at the mandatory levels using radiosonde observations and computed at 12-hour intervals out to 48 hours. Because of known errors associated with radiosonde moisture measurements at high altitudes, the analysis of the upper air dew point temperature verification focuses on levels at and below 500 hPa. Bias and bias-corrected root-mean-square-error (BCRMSE) were computed separately for surface and upper air observations. The CIs were computed from the standard error estimates about the median value of the stratified results using a parametric method and a correction for first-order autocorrelation.

4.2 Precipitation

For the QPF verification, a grid-to-grid comparison was made by first bilinearly interpolating the precipitation analyses to the 15-km model integration domain. This regridded analysis was then used to evaluate the forecast. Accumulation periods of 3 and 24 hours were examined. The observational datasets used were the NCEP Stage II analysis for the 3-hour accumulation and the NCEP/Climate Prediction Center daily gauge analysis for the 24-hour accumulation. Because the 24-hour accumulation observations are only valid at 12 UTC, the 24-hour QPF were examined for the 24- and 48-hour lead times for the 12 UTC initializations and 36-hour lead time for the 00 UTC initializations. Traditional verification metrics computed included the GSS and frequency bias. For the precipitation statistics, a bootstrapping CI method was applied.

4.3 GO Index

Skill scores (S) were computed for wind speed (at 250 hPa, 400 hPa, 850 hPa and surface), dew point temperature (at 400 hPa, 700 hPa, 850 hPa and surface), temperature (at 400 hPa and surface), height (at 400 hPa), and mean sea level pressure, using root-mean-square-error (RMSE) for both the AFWA and RRTMG configurations using the formula:

$$S = 1 - \frac{(RMSE_{RRTMG})^2}{(RMSE_{AFWA})^2}$$

For each variable, level, and forecast hour, predefined weights (w_i), shown in the table below, were then applied and a weighted sum, S_w , was computed

Variable	Level	Weights by lead time			
		12 h	24 h	36 h	48 h
Wind Speed	250 hPa	4	3	2	1
	400 hPa	4	3	2	1
	850 hPa	4	3	2	1
	Surface	8	6	4	2
Dew Point Temperature	400 hPa	8	6	4	2
	700 hPa	8	6	4	2
	850 hPa	8	6	4	2
	Surface	8	6	4	2
Temperature	400 hPa	4	3	2	1
	Surface	8	6	4	2
Height	400 hPa	4	3	2	1
Pressure	Mean sea level	8	6	4	2

where,

$$S_w = \frac{1}{\sum_i w_i} \left(\sum_i (w_i S_i) \right)$$

Once the weighted sum of the skill scores, S_w , was computed, the Index value (N) is defined as:

$$N = \sqrt{\frac{1}{1 - S_w}}$$

Given this definition, which is based on the General Operations (GO) Index, values (N) less than one indicate the AFWA configuration has higher skill and values greater than one indicate the RRTMG configuration has higher skill.

5. Verification Results

Differences are computed between the two configurations by subtracting the RRTMG configuration from the AFWA configuration. BCRMSE is always a positive quantity and a perfect score is zero. Given these properties, differences that are negative (positive) indicate the AFWA (RRTMG) configuration has a lower BCRMSE and is favored. For GSS, the perfect score is one and the no-skill forecast is zero. Thus, if the pair-wise difference is positive (negative) the AFWA (RRTMG) configuration has a higher GSS and is favored. The properties of bias (which has a perfect score of zero) are not as conducive to generalized statements such as those that can be made for BCRMSE and GSS. Bias can have positive or negative values. Given this, when looking at the pair-wise differences it is important to also note the magnitude of the bias in relation to the perfect score for each individual configuration to know which configuration has a smaller bias and is, thus, favored. A breakdown of the configuration with SS and PS better performance by variable, season, statistic, initialization hour, forecast lead time, and level is summarized in Tables 1-8, where the favored configuration is highlighted. Please note, all verification plots generated (by plot type, metric, lead time, threshold, season, etc.) can be viewed on the DTC webpage.

5.1 Upper Air

5.1.1 Temperature BCRMSE and bias

Both the AFWA and RRTMG configurations, regardless of forecast lead time or temporal aggregation, have a minimum in BCRMSE values between 500 and 300 hPa with the largest errors at both the near-surface and upper levels (Fig. 4). For all vertical levels, there is error growth with lead time. Most lead times and vertical levels at and below 300 hPa display SS pair-wise differences, all favoring the RRTMG configuration; the summer aggregation displays the fewest SS pair-wise differences (see Table 1). Only a few SS pair-wise differences favor the AFWA configuration, all of which are observed at or above 200 hPa. None of the SS pair-wise differences for temperature BCRMSE are PS.

Both configurations have a cold bias at 850 hPa, for all temporal aggregations and lead times, which transitions to a warm bias with height (Fig. 5). The level of the transition occurs near or below 500 hPa but is dependent on configuration, seasonal aggregation, and lead time. An exception is noted at the 150 hPa level, which exhibits no bias (CIs encompass zero) or a cold bias for several seasonal aggregations. In general, from 850 – 700 hPa, the AFWA configuration has a larger cold bias than the RRTMG configuration, with many of the differences being PS (see Table 1). At the upper-levels, the SS favored configuration is dependent on the level and temporal aggregation, with only a few having PS.

5.1.2 Dew Point Temperature BCRMSE and bias

The overall distribution of dew point temperature BCRMSE increases as pressure decreases and lead time increases for both configurations and all temporal aggregations (Fig. 6) except winter, where median BCRMSE values decrease from 700 hPa to 500 hPa level (not shown). All SS pair-wise differences show RRTMG as the favored configuration, with a majority of differences being PS; the most SS/PS pair-wise differences occur at 850 hPa (see Table 2).

For all temporal aggregations except summer, a high bias is observed for both configurations at all vertical levels and forecast lead times (Fig. 7). The summer aggregation has a cold bias at 700 hPa for the 24 – 48 hour lead times and generally has an unbiased forecast at 850 hPa. Most pair-wise differences are PS and favor the AFWA configuration, with exception to the summer aggregation, where the RRTMG configuration is consistently favored at 700 hPa.

5.1.3 Wind BCRMSE and bias

In general, both configurations have a very similar distribution of BCRMSE in the vertical for all temporal aggregations and lead times. The lowest errors for wind speed BCRMSE are typically seen at the 850 or 700 hPa level with errors increasing to a maximum around 300 or 200 hPa level before decreasing again further aloft (Fig. 8). A number of SS pair-wise differences are noted, with all but one favoring the RRTMG configuration; however, the magnitude of the differences is small, with none being PS (see Table 3).

For several lead times, both configurations have unbiased forecasts (i.e., the CIs encompass zero) at 850 hPa for all temporal aggregations; with height, the wind speed bias generally becomes more negative (i.e., the winds become too weak) up to the 200 hPa, where the largest magnitude bias is noted (Fig. 9). Above 200 hPa, the bias values become less negative, and at certain forecast lead times, the forecasts become unbiased or even display a high bias. In general, at most vertical levels and lead times, the AFWA configuration has higher (i.e., in most cases, less negative) median bias values than the RRTMG configuration. There are a number of SS pair-wise differences, with the AFWA configuration being a better overall performer; however, there are, again, no PS pair-wise differences (see Table 3).

5.2 Surface

5.2.1 Temperature BCRMSE and bias

The surface temperature BCRMSE displays a general increase with lead time for both the 00 and 12 UTC initializations and for all seasonal aggregations (Fig. 10). In addition, a diurnal signal is noted, with the strength of the signal dependent on the seasonal aggregation. For the annual aggregation, the lowest BCRMSE values occur at times valid around 06 – 09 UTC, while the largest error values are seen at times valid around 15 UTC. A number of SS and PS pair-wise differences are seen for both initializations dependent on temporal aggregation and lead time (see Table 4). Overall, these SS differences favor the RRTMG configuration more often, and all PS pair-wise differences favor the RRTMG configuration.

A diurnal cycle is evident in surface temperature bias, for both configurations, both initializations, and all temporal aggregations (Fig. 11). In general, a SS cold bias is observed at a majority of forecast lead times for both 00 and 12 UTC initializations. A few exceptions include several unbiased forecasts and a few warm biased forecasts valid between 06 and 12 UTC for the annual and winter aggregations. The often observed cold bias is strongest at times valid near 15 – 00 UTC (i.e., during the daytime) for both configurations. The RRTMG configuration has a PS smaller bias than the AFWA configuration for most lead times and temporal aggregation (see Table 4). The only notable exception is for times valid from 06 – 12 UTC during the winter aggregation, where the PS differences favor the AFWA configuration.

5.2.2 Dew Point Temperature BCRMSE and bias

Similar to surface temperature BCRMSE, an increase in dew point temperature BCRMSE is noted with lead time, for both initializations and all temporal aggregations (Fig. 12); a diurnal trend is noted in all but the fall aggregation. The magnitude of the differences between the configurations is small, leading to a number of SS pair-wise differences (see Table 5). A general diurnal trend is observed in which configuration is favored. SS pair-wise differences typically favor the AFWA configuration during the afternoon/early evening, while the RRTMG configuration is a better performer during the overnight/early morning; however, the strength of the trend is dependent on the initialization time and temporal aggregation. While there are many SS pair-wise differences, only one is PS.

The time series of dew point temperature bias is sensitive to temporal aggregation and forecast lead time for both configurations. A diurnal trend is noted for both configurations, both initializations and all temporal aggregations, with the spring and summer aggregations exhibiting the largest amplitude and winter having the smallest (Fig. 13). The winter aggregation has a high bias for all forecasts, regardless of initialization time. For the annual, spring, and summer aggregations, both configurations have a general high bias for forecasts valid between 18 – 00 UTC. A low bias is noted for most forecasts between valid between 06 – 12 UTC for the summer aggregation. For both initializations, all temporal aggregations, and most lead times, the AFWA configuration has drier median bias values than the RRTMG configuration leading to better performance during the afternoon/evening when a high bias is noted and worse during the overnight/early morning hours when a low bias is noted. Most pair-wise differences between the two configurations are PS; in general, however, the AFWA configuration has more PS pair-wise differences than the RRTMG configuration (see Table 5).

5.2.3 Wind BCRMSE and bias

A diurnal signal in wind speed BCRMSE is noted for both configurations and all temporal aggregations except winter; in addition, an increase in surface wind speed BCRMSE with forecast lead time is seen (Fig. 14). For the 00 and 12 UTC initializations and for all temporal aggregations, both configurations have the smallest wind speed errors around 12 UTC, while the largest errors occur around 00 UTC. The differences between the two configurations are small in

magnitude; several SS pair-wise differences are seen, of which all but two favor the RRTMG configuration, with no PS differences noted (see Table 6).

A high wind speed bias is observed for both configurations at nearly all forecast lead times, regardless of initialization time or temporal aggregation (Fig. 15). In addition, a prominent diurnal trend is noted; for both configurations, a SS larger high bias is typically seen during the overnight hours as compared to the daytime hours. A majority of lead times show the AFWA configuration as the SS better performer; the only exception is at select forecast lead times valid at 12 UTC, where there are either no SS pair-wise differences or the RRTMG configuration is favored (see Table 6). No PS pair-wise differences are noted.

5.2.4 3-hourly QPF GSS and bias

For all configurations, initializations, and forecast lead times, as the threshold increases from 0.01" to 1.0", the GSS steadily decreases (Fig. 16). Similar behavior is seen in the base rate, which is a measure of the observed grid box events to the total number of grid boxes in the domain. Overall, the highest base rates are seen during the summer season, regardless of threshold, and at the lowest thresholds, regardless of season. Lower base rates are typically present at the higher thresholds due the infrequency of high-precipitation events, and, therefore, CIs are often larger at thresholds where not as many events occur. Overall, the AFWA and RRTMG configurations perform similarly when considering 3-hourly QPF GSS and only a handful of SS pair-wise differences are seen. Most differences favor the AFWA configuration, with a notable exception seen at several of the lower thresholds during the winter aggregation, which favor the RRMTG configuration (see Table 7).

In general, a SS high bias is seen for all thresholds below 0.25", for both initializations, regardless of forecast lead time and for all temporal aggregations except summer (Fig. 17). For both initializations and several lead times, the annual and summer aggregations transition to a low bias at the higher thresholds, while the winter aggregation has a high bias for most thresholds, with exception to the highest ones, where there are generally large CIs encompassing the median value. There are no SS pair-wise differences, indicating both configurations perform comparatively.

5.2.5 Daily Precipitation GSS and bias

Similar to the 3-hourly QPF, GSS tends to decrease with increasing thresholds for both configurations, both initialization times, most lead times, and all temporal aggregations (Fig. 18). The base rate decreases with increasing threshold, with very few observed events at the highest thresholds; therefore, the width of the CIs also tends to increase with increasing threshold, with the winter aggregation having the largest CIs. Table 8 shows at the 0.01" threshold, all SS pair-wise differences favor the RRTMG configuration. For all other thresholds, SS pair-wise differences favor the AFWA configuration.

Both configurations generally have a high bias for both initializations and all lead times at all but the highest thresholds, where the CIs often encompass one (Fig. 19). In addition, for the fall and winter aggregations, the CIs occasionally encompass one at the middle-range thresholds as well. For frequency bias for daily QPF, there are no SS pair-wise differences between the two configurations.

5.3 GO Index

Regardless of initialization or temporal aggregation, the GO Index median values and associated CIs, indicated by the width of the notches on the boxplot, were greater than one, indicating the RRTMG configuration is more skillful than the AFWA configuration (Fig. 20). In general, for both the 00 and 12 UTC initializations, the fall aggregation displays the highest median values, while the winter aggregation has the lowest median values. The largest variability is seen in the annual

and spring aggregations, and the 00 UTC initializations typically have less variability than the 12 UTC initializations.

6. Summary

For this end-to-end sensitivity test, two WRF-ARW configurations were tested and evaluated; one configuration employed AFWA's OC, which was used as a baseline, and the other configuration replaced AFWA's long- and short-wave radiation schemes with the RRTMG schemes, in hopes of assessing potential impacts of the performance of the scheme. In addition to evaluating performance, computational efficiency of the two configurations was also investigated; on average, there was a 27% increase in CPU time required to run the RRTMG configuration as compared to the AFWA configuration.

Due to the nature of the testing methodology (i.e., running both configurations over an identical set of cases), pair-wise differences were computed for several verification metrics; in addition, an assessment of SS and PS was completed. Overall, there were a large number SS and PS pair-wise differences between the two configurations, with there being a sensitivity in which configuration was favored based on verification metric, temporal aggregation, initialization time, vertical level, lead time, and threshold. In general, however, more PS pair-wise differences indicated the RRTMG configuration out-performs the AFWA configuration. This result is also reflected in the GO Index, where the RRTMG configuration was consistently the better performer of the two configurations, regardless of initialization time or temporal aggregation.

7. References

Iacono, M.J., J.S. Delamere, E.J. Mlawer, M.W. Shephard, S.A. Clough, and W.D. Collins, 2008: Radiative forcing by long-lived greenhouse gases: Calculations with the AER radiative transfer models, *J. Geophys. Res.*, **113**, D13103.

Skamarock, W. C., J. B. Klemp, J. Dudhia, D. O. Gill, D. M. Barker, W. Wang and J. G. Powers, 2008: A Description of the Advanced Research WRF Version 3, NCAR Tech Note, NCAR/TN-475+STR, 113 pp.

Table 1. SS (light shading) and PS (dark shading) pair-wise differences between the AFWA and RRTMG configurations run with WRF v3.3.1 (where the highlighted configuration is favored) for upper air temperature BCRMSE and bias by pressure level, season, and forecast lead time for the 00 UTC and 12 UTC initializations combined over the full integration domain.

Upper Air Temperature		Annual				Summer				Fall				Winter				Spring			
		f12	f24	f36	f48	f12	f24	f36	f48	f12	f24	f36	f48	f12	f24	f36	f48	f12	f24	f36	f48
BCRMSE	850	RRTMG	RRTMG	RRTMG	RRTMG	RRTMG	RRTMG	--	RRTMG	--	RRTMG	RRTMG	RRTMG	RRTMG	RRTMG	RRTMG	RRTMG	RRTMG	--	RRTMG	RRTMG
	700	RRTMG	RRTMG	RRTMG	RRTMG	RRTMG	RRTMG	RRTMG	RRTMG	RRTMG	RRTMG	RRTMG	RRTMG	RRTMG	RRTMG	RRTMG	RRTMG	RRTMG	RRTMG	RRTMG	RRTMG
	500	--	RRTMG	RRTMG	RRTMG	--	--	--	--	--	RRTMG	RRTMG	RRTMG	--	RRTMG	RRTMG	RRTMG	RRTMG	RRTMG	RRTMG	RRTMG
	400	RRTMG	RRTMG	RRTMG	RRTMG	--	--	--	--	RRTMG	RRTMG	RRTMG	RRTMG	RRTMG	RRTMG	RRTMG	RRTMG	--	RRTMG	RRTMG	RRTMG
	300	RRTMG	RRTMG	RRTMG	RRTMG	RRTMG	RRTMG	--	--	RRTMG	RRTMG	RRTMG	RRTMG	RRTMG	RRTMG	RRTMG	RRTMG	RRTMG	RRTMG	RRTMG	RRTMG
	200	--	--	AFWA	--	--	--	--	--	--	--	--	--	--	--	--	--	--	--	--	--
	150	--	--	--	--	--	AFWA	AFWA	AFWA	--	--	--	--	--	--	--	--	--	--	--	--
	100	RRTMG	--	AFWA	--	--	--	--	--	--	--	AFWA	--	RRTMG	--	--	--	--	--	AFWA	--
Bias	850	--	RRTMG	RRTMG	RRTMG	RRTMG	RRTMG	RRTMG	RRTMG	--	RRTMG	RRTMG	RRTMG	--	RRTMG	RRTMG	RRTMG	--	RRTMG	RRTMG	RRTMG
	700	--	RRTMG	RRTMG	RRTMG	RRTMG	RRTMG	RRTMG	RRTMG	--	RRTMG	RRTMG	RRTMG	--	RRTMG	RRTMG	RRTMG	--	RRTMG	RRTMG	RRTMG
	500	--	AFWA	AFWA	AFWA	AFWA	AFWA	AFWA	AFWA	--	AFWA	AFWA	AFWA	--	--	RRTMG	RRTMG	--	AFWA	AFWA	AFWA
	400	--	--	AFWA	AFWA	RRTMG	RRTMG	--	--	--	--	--	AFWA	AFWA	AFWA	AFWA	AFWA	RRTMG	--	AFWA	AFWA
	300	--	--	RRTMG	--	RRTMG	RRTMG	RRTMG	RRTMG	--	--	--	--	AFWA	AFWA	AFWA	AFWA	--	--	--	--
	200	--	RRTMG	RRTMG	RRTMG	--	--	--	--	--	RRTMG	RRTMG	RRTMG	RRTMG	RRTMG	RRTMG	RRTMG	--	RRTMG	RRTMG	RRTMG
	150	AFWA	AFWA	RRTMG	RRTMG	AFWA	AFWA	AFWA	AFWA	AFWA	AFWA	--	AFWA	--	--	--	--	RRTMG	--	--	--
	100	AFWA	AFWA	AFWA	AFWA	AFWA	AFWA	AFWA	AFWA	AFWA	--	--	--	--	--	--	--	AFWA	AFWA	AFWA	AFWA

Table 2. SS (light shading) and PS (dark shading) pair-wise differences between the AFWA and RRTMG configurations run with WRF v3.3.1 (where the highlighted configuration is favored) for upper air dew point temperature BCRMSE and bias by pressure level, season, and forecast lead time for the 00 UTC and 12 UTC initializations combined over the full integration domain.

Upper Air Dew Point Temperature		Annual				Summer				Fall				Winter				Spring			
		f12	f24	f36	f48	f12	f24	f36	f48	f12	f24	f36	f48	f12	f24	f36	f48	f12	f24	f36	f48
BCRMSE	850	RRTMG	RRTMG	RRTMG	RRTMG	--	--	RRTMG	RRTMG	--	RRTMG	RRTMG	RRTMG	RRTMG	--	RRTMG	--	--	--	RRTMG	--
	700	RRTMG	--	--	--	--	--	--	--	--	--	--	--	RRTMG	RRTMG	--	--	--	--	--	--
	500	--	--	--	--	--	--	--	RRTMG	--	--	--	--	--	--	--	--	--	RRTMG	--	--
Bias	850	AFWA	AFWA	AFWA	AFWA	AFWA	AFWA	AFWA	RRTMG	--	AFWA	AFWA	AFWA	--	AFWA	AFWA	AFWA	AFWA	AFWA	AFWA	AFWA
	700	AFWA	AFWA	AFWA	AFWA	RRTMG	RRTMG	RRTMG	RRTMG	AFWA	AFWA	AFWA	AFWA	AFWA	AFWA	AFWA	AFWA	AFWA	AFWA	AFWA	AFWA
	500	AFWA	AFWA	AFWA	AFWA	AFWA	AFWA	AFWA	AFWA	AFWA	AFWA	AFWA	AFWA	AFWA	AFWA	AFWA	AFWA	AFWA	AFWA	AFWA	AFWA

Table 3. SS (light shading) and PS (dark shading) pair-wise differences between the AFWA and RRTMG configurations run with WRF v3.3.1 (where the highlighted configuration is favored) for upper air wind BCRMSE and bias by pressure level, season, and forecast lead time for the 00 UTC and 12 UTC initializations combined over the full integration domain.

Upper Air Wind Speed		Annual				Summer				Fall				Winter				Spring			
		f12	f24	f36	f48	f12	f24	f36	f48	f12	f24	f36	f48	f12	f24	f36	f48	f12	f24	f36	f48
BCRMSE	850	RRTMG	RRTMG	RRTMG	RRTMG	--	--	--	--	--	--	RRTMG	RRTMG	RRTMG	RRTMG	RRTMG	--	--	--	--	--
	700	--	RRTMG	RRTMG	--	--	--	--	--	--	RRTMG	--	--	--	RRTMG	RRTMG	--	--	--	--	--
	500	--	RRTMG	RRTMG	RRTMG	--	--	--	--	--	--	RRTMG	--	--	--	RRTMG	--	--	RRTMG	RRTMG	RRTMG
	400	RRTMG	RRTMG	RRTMG	RRTMG	RRTMG	--	RRTMG	RRTMG	--	RRTMG	--	RRTMG	RRTMG	RRTMG	RRTMG	RRTMG	RRTMG	RRTMG	RRTMG	RRTMG
	300	RRTMG	RRTMG	RRTMG	RRTMG	--	RRTMG	--	--	RRTMG	RRTMG	RRTMG	RRTMG	--	--	RRTMG	RRTMG	--	RRTMG	RRTMG	--
	200	--	--	RRTMG	--	--	RRTMG	--	--	--	--	--	--	--	--	--	--	--	--	--	--
	150	RRTMG	--	--	--	RRTMG	--	--	--	RRTMG	--	--	--	--	--	--	--	--	--	--	AFWA
	100	--	--	--	--	--	--	--	--	--	--	--	--	--	--	--	--	--	--	--	RRTMG
Bias	850	AFWA	RRTMG	--	--	--	AFWA	AFWA	AFWA	AFWA	RRTMG	RRTMG	RRTMG	AFWA	AFWA	AFWA	RRTMG	--	--	--	--
	700	AFWA	AFWA	AFWA	AFWA	--	--	--	--	AFWA	AFWA	AFWA	AFWA	--	AFWA	AFWA	AFWA	--	AFWA	--	AFWA
	500	--	AFWA	AFWA	AFWA	--	--	--	--	--	--	--	AFWA	--	--	AFWA	AFWA	--	AFWA	AFWA	--
	400	AFWA	AFWA	AFWA	AFWA	--	--	--	--	--	--	AFWA	AFWA	AFWA	AFWA	AFWA	AFWA	AFWA	--	AFWA	AFWA
	300	AFWA	AFWA	AFWA	AFWA	AFWA	AFWA	AFWA	AFWA	AFWA	AFWA	AFWA	AFWA	AFWA	AFWA	AFWA	AFWA	AFWA	AFWA	AFWA	AFWA
	200	AFWA	AFWA	AFWA	AFWA	AFWA	AFWA	AFWA	--	AFWA	AFWA	AFWA	AFWA	AFWA	AFWA	AFWA	AFWA	AFWA	AFWA	AFWA	AFWA
	150	AFWA	AFWA	AFWA	AFWA	--	--	--	--	AFWA	AFWA	AFWA	AFWA	AFWA	AFWA	RRTMG	RRTMG	AFWA	AFWA	AFWA	AFWA
	100	--	--	RRTMG	--	--	RRTMG	RRTMG	RRTMG	--	--	--	--	--	--	--	--	--	--	--	--

Table 4. SS (light shading) and PS (dark shading) pair-wise differences between the AFWA and RRTMG configurations run with WRF v3.3.1 (where the highlighted configuration is favored) for surface temperature BCRMSE and bias by season and forecast lead time for the 00 UTC and 12 UTC initializations separately over the full integration domain.

Surface Temperature		f03	f06	f09	f12	f15	f18	f21	f24	f27	f30	f33	f36	f39	f42	f45	f48		
BCRMSE	00 UTC Initializations	Annual	RRTMG	--	AFWA	--	RRTMG	--	--	RRTMG	--	--	--	RRTMG	RRTMG	RRTMG	--	RRTMG	
		Summer	RRTMG	--	--	RRTMG	RRTMG	AFWA	AFWA	--	RRTMG	--	RRTMG	RRTMG	--	--	--	--	RRTMG
		Fall	RRTMG	--	AFWA	--	RRTMG	RRTMG	RRTMG	RRTMG	--	--	--	--	RRTMG	RRTMG	RRTMG	RRTMG	RRTMG
		Winter	RRTMG	--	AFWA	AFWA	--	RRTMG	RRTMG	RRTMG	--	--	--	--	RRTMG	RRTMG	RRTMG	RRTMG	RRTMG
		Spring	--	--	--	--	RRTMG	--	--	--	--	--	--	--	RRTMG	--	--	--	--
	12 UTC Initializations	Annual	--	--	--	RRTMG	--	--	--	--	RRTMG	RRTMG	--	RRTMG	RRTMG	RRTMG	--	--	RRTMG
		Summer	--	--	AFWA	--	RRTMG	RRTMG	--	RRTMG	RRTMG	--	--	RRTMG	RRTMG	RRTMG	RRTMG	RRTMG	RRTMG
		Fall	RRTMG	--	--	RRTMG	RRTMG	--	--	--	RRTMG	RRTMG	--	RRTMG	--	--	RRTMG	RRTMG	RRTMG
		Winter	RRTMG	--	RRTMG	RRTMG	--	AFWA	AFWA	--	RRTMG	RRTMG	RRTMG	RRTMG	RRTMG	--	--	--	--
		Spring	--	AFWA	AFWA	--	AFWA	AFWA	AFWA	--	--	--	--	--	--	--	--	AFWA	--
Bias	00 UTC Initializations	Annual	--	--	--	--	RRTMG	RRTMG	RRTMG	RRTMG	RRTMG	RRTMG	RRTMG	RRTMG	RRTMG	RRTMG	RRTMG	RRTMG	
		Summer	RRTMG	RRTMG	--	RRTMG	RRTMG	RRTMG	RRTMG	RRTMG	RRTMG	RRTMG	RRTMG	RRTMG	RRTMG	RRTMG	RRTMG	RRTMG	RRTMG
		Fall	--	--	--	--	RRTMG	RRTMG	RRTMG	RRTMG	RRTMG	RRTMG	RRTMG	RRTMG	RRTMG	RRTMG	RRTMG	RRTMG	RRTMG
		Winter	AFWA	AFWA	RRTMG	RRTMG	RRTMG	RRTMG	RRTMG	RRTMG	RRTMG	AFWA	AFWA	AFWA	RRTMG	RRTMG	RRTMG	RRTMG	RRTMG
		Spring	--	--	AFWA	--	RRTMG	RRTMG	RRTMG	RRTMG	RRTMG	RRTMG	RRTMG	RRTMG	RRTMG	RRTMG	RRTMG	RRTMG	RRTMG
	12 UTC Initializations	Annual	RRTMG	RRTMG	RRTMG	RRTMG	RRTMG	RRTMG	RRTMG	RRTMG	RRTMG	RRTMG	RRTMG	RRTMG	RRTMG	RRTMG	RRTMG	RRTMG	RRTMG
		Summer	RRTMG	RRTMG	RRTMG	RRTMG	RRTMG	RRTMG	RRTMG	RRTMG	RRTMG	RRTMG	RRTMG	RRTMG	RRTMG	RRTMG	RRTMG	RRTMG	RRTMG
		Fall	RRTMG	RRTMG	RRTMG	RRTMG	RRTMG	RRTMG	RRTMG	RRTMG	RRTMG	RRTMG	RRTMG	RRTMG	RRTMG	RRTMG	RRTMG	RRTMG	RRTMG
		Winter	RRTMG	RRTMG	RRTMG	RRTMG	RRTMG	AFWA	AFWA	AFWA	RRTMG	RRTMG	RRTMG	RRTMG	RRTMG	RRTMG	AFWA	AFWA	AFWA
		Spring	RRTMG	RRTMG	RRTMG	RRTMG	RRTMG	RRTMG	RRTMG	RRTMG	RRTMG	RRTMG	RRTMG	RRTMG	RRTMG	RRTMG	RRTMG	RRTMG	RRTMG

Table 5. SS (light shading) and PS (dark shading) pair-wise differences between the AFWA and RRTMG configurations run with WRF v3.3.1 (where the highlighted configuration is favored) for surface dew point temperature BCRMSE and bias by season and forecast lead time for the 00 UTC and 12 UTC initializations separately over the full integration domain.

Surface Dew Point Temperature		f03	f06	f09	f12	f15	f18	f21	f24	f27	f30	f33	f36	f39	f42	f45	f48		
BCRMSE	00 UTC Initializations	Annual	RRTMG	RRTMG	RRTMG	RRTMG	RRTMG	AFWA	AFWA	AFWA	--	RRTMG	RRTMG	RRTMG	--	--	AFWA	AFWA	
		Summer	RRTMG	RRTMG	RRTMG	RRTMG	--	AFWA	AFWA	AFWA	--	--	RRTMG	RRTMG	AFWA	AFWA	AFWA	AFWA	
		Fall	RRTMG	RRTMG	RRTMG	RRTMG	RRTMG	--	--	--	--	--	--	--	RRTMG	--	--	--	
		Winter	RRTMG	--	--	--	--	AFWA	AFWA	--	--	--	--	--	--	--	--	--	
		Spring	AFWA	--	--	--	--	AFWA	AFWA	AFWA	--	--	--	RRTMG	--	--	--	--	
	12 UTC Initializations	Annual	--	AFWA	AFWA	AFWA	AFWA	--	RRTMG	RRTMG	--	AFWA	AFWA	AFWA	--	RRTMG	RRTMG	RRTMG	
		Summer	--	AFWA	AFWA	AFWA	--	RRTMG	RRTMG	RRTMG	AFWA	AFWA	AFWA	AFWA	--	RRTMG	RRTMG	RRTMG	
		Fall	RRTMG	--	--	AFWA	--	--	--	--	RRTMG	--	--	--	--	RRTMG	RRTMG	RRTMG	
		Winter	--	AFWA	AFWA	--	--	--	--	RRTMG	RRTMG	--	AFWA	--	--	--	--	--	
		Spring	--	--	AFWA	AFWA	AFWA	--	--	--	--	AFWA	AFWA	AFWA	--	AFWA	--	--	
Bias	00 UTC Initializations	Annual	--	--	--	--	AFWA	AFWA	AFWA	AFWA	AFWA	AFWA	AFWA	RRTMG	AFWA	AFWA	AFWA	AFWA	
		Summer	RRTMG	RRTMG	--	RRTMG	AFWA	AFWA	AFWA	AFWA	RRTMG	RRTMG	RRTMG	RRTMG	AFWA	AFWA	AFWA	AFWA	
		Fall	--	--	--	--	RRTMG	AFWA	AFWA	RRTMG	RRTMG	RRTMG	RRTMG	RRTMG	RRTMG	AFWA	AFWA	RRTMG	
		Winter	RRTMG	RRTMG	RRTMG	RRTMG	--	AFWA	AFWA	AFWA	AFWA	AFWA	AFWA	AFWA	AFWA	AFWA	AFWA	AFWA	
		Spring	--	--	--	--	AFWA	AFWA	AFWA	AFWA	AFWA	AFWA	AFWA	RRTMG	AFWA	AFWA	AFWA	AFWA	
	12 UTC Initializations	Annual	AFWA	--	--	AFWA	AFWA	AFWA	AFWA	RRTMG	AFWA	AFWA	AFWA	AFWA	AFWA	AFWA	AFWA	AFWA	RRTMG
		Summer	RRTMG	AFWA	AFWA	AFWA	RRTMG	RRTMG	RRTMG	RRTMG	AFWA	AFWA	AFWA	AFWA	RRTMG	RRTMG	RRTMG	RRTMG	RRTMG
		Fall	RRTMG	AFWA	AFWA	AFWA	RRTMG	RRTMG	RRTMG	RRTMG	RRTMG	AFWA	AFWA	AFWA	RRTMG	AFWA	AFWA	RRTMG	
		Winter	AFWA	AFWA	AFWA	AFWA	AFWA	AFWA	AFWA	AFWA	AFWA	AFWA	AFWA	AFWA	AFWA	AFWA	AFWA	AFWA	AFWA
		Spring	AFWA	AFWA	AFWA	AFWA	AFWA	AFWA	AFWA	RRTMG	AFWA	AFWA	AFWA	AFWA	AFWA	AFWA	AFWA	AFWA	RRTMG

Table 6. SS differences between the AFWA and RRTMG configurations run with WRF v3.3.1 (where the highlighted configuration is favored) for surface wind BCRMSE and bias by season and forecast lead time for the 00 UTC and 12 UTC initializations separately over the full integration domain.

Surface Wind Speed		f03	f06	f09	f12	f15	f18	f21	f24	f27	f30	f33	f36	f39	f42	f45	f48	
BCRMSE	00 UTC Initializations	Annual	RRTMG	RRTMG	RRTMG	RRTMG	RRTMG	RRTMG	RRTMG	RRTMG	RRTMG	RRTMG	RRTMG	RRTMG	RRTMG	RRTMG	RRTMG	RRTMG
		Summer	RRTMG	RRTMG	RRTMG	RRTMG	RRTMG	--	--	--	--	--	--	RRTMG	--	--	--	--
		Fall	RRTMG	RRTMG	RRTMG	RRTMG	RRTMG	RRTMG	RRTMG	RRTMG	--	RRTMG	RRTMG	RRTMG	RRTMG	RRTMG	--	RRTMG
		Winter	--	--	RRTMG	RRTMG	RRTMG	RRTMG	RRTMG	RRTMG	--	RRTMG	RRTMG	--	RRTMG	RRTMG	RRTMG	RRTMG
		Spring	RRTMG	--	--	RRTMG	--	--	RRTMG	RRTMG	RRTMG	--	--	--	RRTMG	RRTMG	RRTMG	--
	12 UTC Initializations	Annual	RRTMG	RRTMG	--	RRTMG	RRTMG	--	--	RRTMG	RRTMG	RRTMG	RRTMG	RRTMG	RRTMG	RRTMG	--	RRTMG
		Summer	AFWA	--	AFWA	RRTMG	RRTMG	--	--	RRTMG	--	--	--	--	--	--	--	RRTMG
		Fall	RRTMG	--	RRTMG	--	--	RRTMG	--	--	RRTMG	RRTMG	RRTMG	RRTMG	RRTMG	--	--	--
		Winter	RRTMG	RRTMG	RRTMG	RRTMG	RRTMG	--	--	RRTMG	RRTMG	RRTMG	RRTMG	RRTMG	RRTMG	RRTMG	RRTMG	RRTMG
		Spring	RRTMG	--	--	RRTMG	--	--	--	--	--	--	--	--	--	--	--	--
Bias	00 UTC Initializations	Annual	AFWA	AFWA	--	RRTMG	AFWA	AFWA	AFWA	AFWA	AFWA	AFWA	--	--	AFWA	AFWA	AFWA	AFWA
		Summer	AFWA	AFWA	AFWA	RRTMG	AFWA	AFWA	AFWA	AFWA	AFWA	AFWA	AFWA	--	AFWA	AFWA	AFWA	AFWA
		Fall	--	--	--	RRTMG	AFWA	AFWA	AFWA	AFWA	--	--	--	RRTMG	--	AFWA	AFWA	AFWA
		Winter	AFWA	--	--	--	--	AFWA	AFWA	AFWA	AFWA	--	--	--	--	AFWA	AFWA	AFWA
		Spring	AFWA	AFWA	--	RRTMG	AFWA	AFWA	AFWA	AFWA	AFWA	AFWA	--	RRMTG	AFWA	AFWA	AFWA	AFWA
	12 UTC Initializations	Annual	AFWA	AFWA	AFWA	AFWA	AFWA	AFWA	AFWA	--	AFWA	AFWA	AFWA	AFWA	AFWA	AFWA	AFWA	--
		Summer	AFWA	AFWA	AFWA	AFWA	AFWA	AFWA	AFWA	--	AFWA	AFWA	AFWA	AFWA	AFWA	AFWA	AFWA	--
		Fall	AFWA	AFWA	AFWA	AFWA	AFWA	AFWA	--	RRTMG	--	AFWA	AFWA	AFWA	AFWA	--	--	--
		Winter	AFWA	AFWA	AFWA	AFWA	AFWA	AFWA	--	--	--	AFWA	AFWA	AFWA	AFWA	--	--	--
		Spring	AFWA	AFWA	AFWA	AFWA	AFWA	AFWA	AFWA	--	AFWA	AFWA	AFWA	AFWA	AFWA	AFWA	AFWA	--

Table 7. SS differences between the AFWA and RRTMG configurations run with WRF v3.3.1 (where the highlighted configuration is favored) for 3-hour QPF GSS by season, forecast lead time, and threshold for the 00 UTC and 12 UTC initializations separately over the full integration domain.

3-hour QPF		00 UTC Initializations									12 UTC Initializations									
		>0.01	>0.02	>0.05	>0.1	>0.15	>0.25	>0.35	>0.5	>1	>0.01	>0.02	>0.05	>0.1	>0.15	>0.25	>0.35	>0.5	>1	
GSS	Annual	f12	--	--	--	--	--	--	--	--	--	--	AFWA	AFWA	AFWA	AFWA	--	AFWA	AFWA	--
		f24	--	AFWA	AFWA	AFWA	--	--	--	--	--	--	--	--	--	--	--	--	--	--
		f36	--	--	--	--	--	--	--	--	--	--	--	--	--	--	--	--	--	--
		f48	--	--	--	--	--	--	--	--	--	--	--	--	--	--	--	--	--	--
	Summer	f12	--	--	AFWA	--	--	--	--	--	--	--	--	AFWA	AFWA	AFWA	--	--	AFWA	--
		f24	--	--	--	--	--	--	--	--	--	--	--	--	--	--	--	--	--	--
		f36	--	--	--	--	--	--	--	--	AFWA	--	--	--	--	--	--	--	--	--
		f48	--	--	--	--	--	--	--	--	--	--	--	--	--	--	--	RRTMG	--	--
	Fall	f12	--	--	--	--	--	--	--	--	--	--	AFWA	AFWA	--	AFWA	--	AFWA	--	--
		f24	--	--	--	--	--	--	--	--	--	--	--	RRTMG	--	--	--	--	--	--
		f36	--	--	--	--	--	--	--	--	--	--	--	--	--	--	--	--	--	AFWA
		f48	--	--	--	--	--	--	--	--	AFWA	--	--	--	--	--	--	--	--	--
	Winter	f12	--	--	--	--	--	--	--	--	--	RRTMG	--	--	--	--	--	--	--	AFWA
		f24	RRTMG	--	--	--	--	--	--	--	--	RRTMG	--	--	--	--	--	--	--	--
		f36	--	--	--	--	--	--	--	--	--	--	--	--	--	--	--	--	--	--
		f48	RRTMG	RRTMG	--	--	--	--	AFWA	--	--	RRTMG	RRTMG	--	--	--	AFWA	--	--	--
Spring	f12	--	--	--	--	--	--	--	AFWA	--	AFWA	AFWA	AFWA	--	--	--	--	--	--	
	f24	AFWA	AFWA	AFWA	--	--	--	--	--	--	--	--	--	--	--	--	--	--	--	
	f36	--	--	--	--	--	--	--	--	--	--	--	--	--	--	--	--	--	--	
	f48	--	AFWA	AFWA	--	--	--	--	--	--	--	--	--	--	--	--	--	--	--	

Table 8. SS differences between the AFWA and RRTMG configurations run with WRF v3.3.1 (where the highlighted configuration is favored) for 24-hour QPF GSS by season, forecast lead time, and threshold for the 00 UTC and 12 UTC initializations separately over the full integration domain.

Daily QPF			>0.01	>0.25	>0.5	>0.75	>1	>1.25	>1.5	>2	>3	
GSS	00 UTC Initializations	Annual	f36	RRTMG	AFWA	AFWA	AFWA	AFWA	--	--	--	--
		Summer	f36	RRTMG	--	--	--	AFWA	AFWA	--	--	--
		Fall	f36	RRTMG	--	--	--	--	--	--	--	--
		Winter	f36	RRTMG	--	--	AFWA	--	--	--	--	--
		Spring	f36	RRTMG	--	--	--	--	--	--	--	--
	12 UTC Initializations	Annual	f24	RRTMG	--	AFWA	AFWA	AFWA	AFWA	AFWA	AFWA	--
			f48	RRTMG	--	--	--	--	--	--	--	--
		Summer	f24	--	--	AFWA	--	--	--	--	--	--
			f48	RRTMG	--	--	--	--	--	--	--	--
		Fall	f24	RRTMG	--	--	AFWA	AFWA	--	--	--	--
			f48	RRTMG	--	--	--	--	--	--	--	--
		Winter	f24	RRTMG	--	--	--	AFWA	--	AFWA	AFWA	--
			f48	RRTMG	--	--	--	--	--	--	--	--
		Spring	f24	RRTMG	AFWA	AFWA	--	AFWA	AFWA	--	--	--
f48	--		--	--	--	--	--	--	--	--		

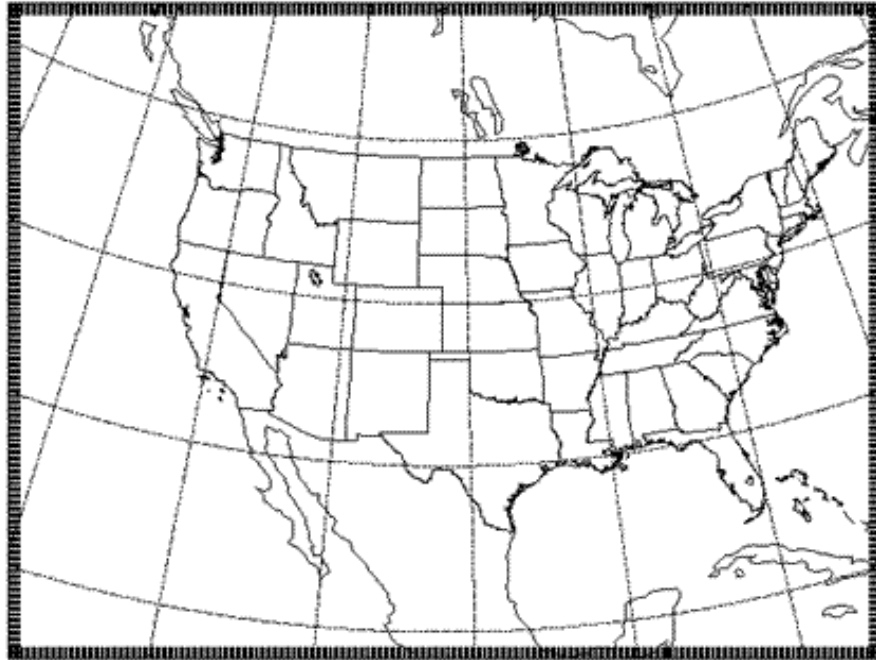


Figure 1. WRF-ARW computational domain.

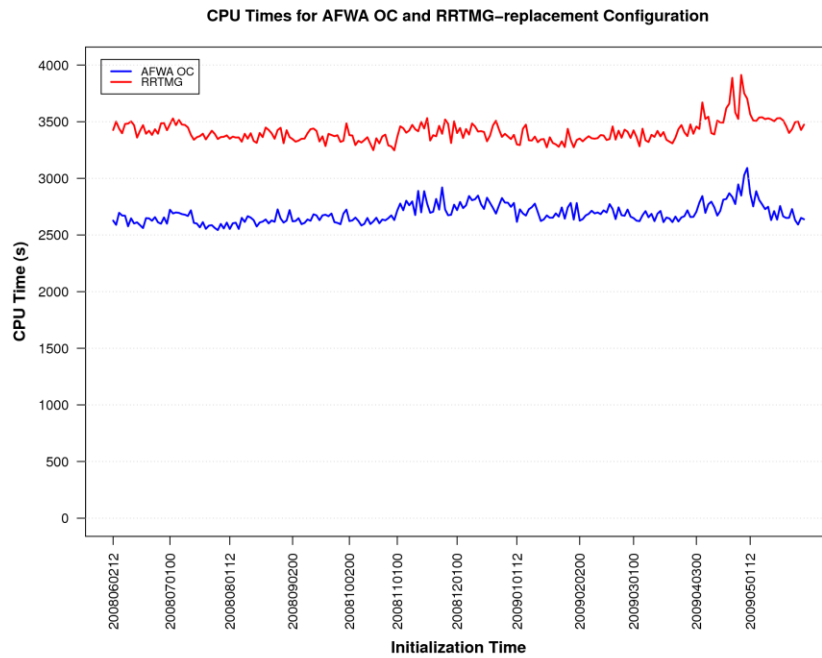


Figure 2. Time series of WRFv3.3.1 run times (s) for all initializations used in this test. The first initialization time is 2008060212, and the final initialization time is 2009053112; forecasts were initialized every 36 hours and run out to 48 hours. The AFWA configuration is in blue, and the RRTMG configuration is in red.

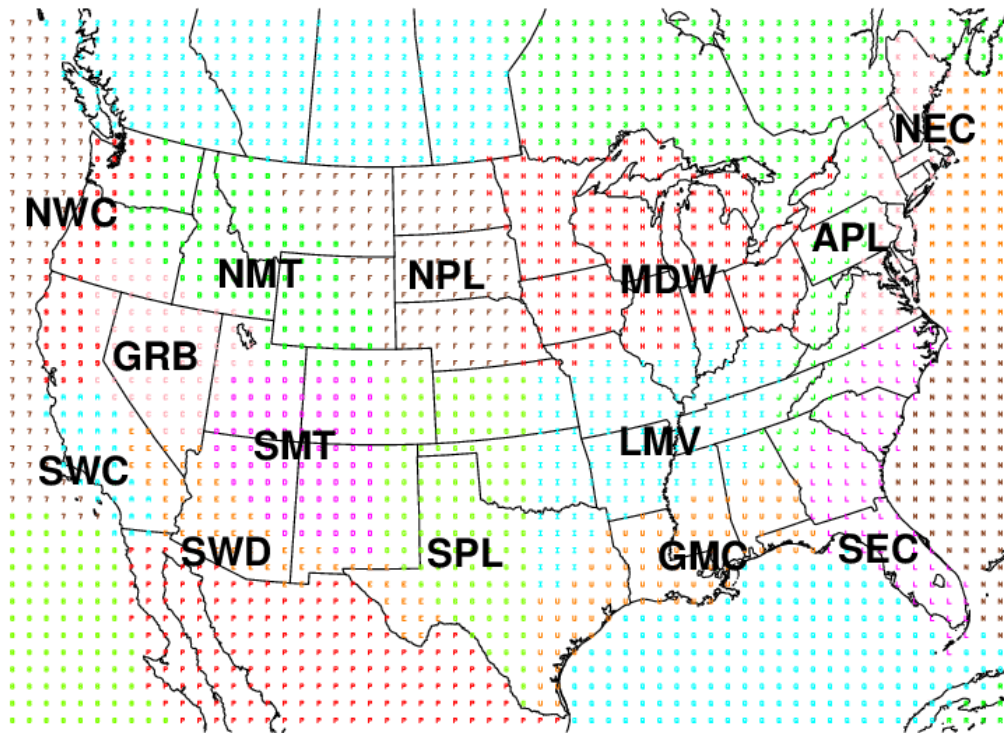
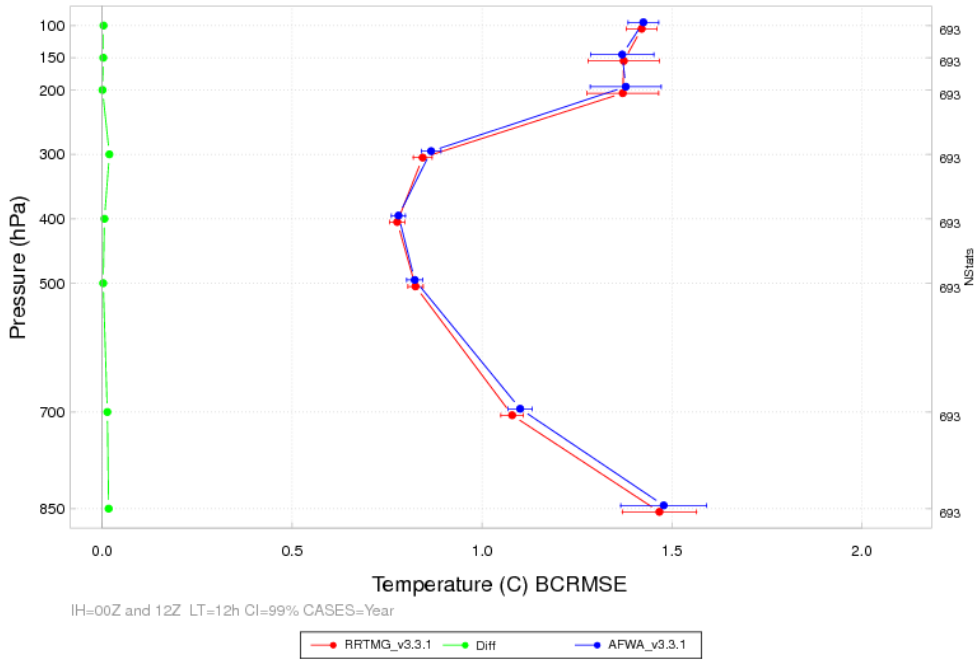


Figure 3. Boundaries of the 14 regional verification domains.

(a) LT=12 h



(b) LT=48 h

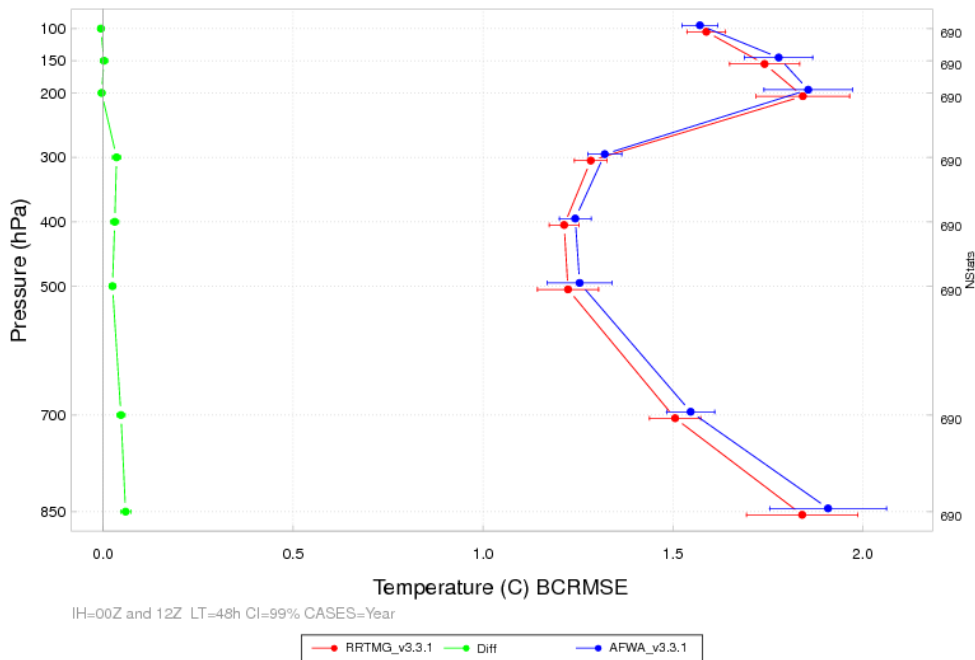
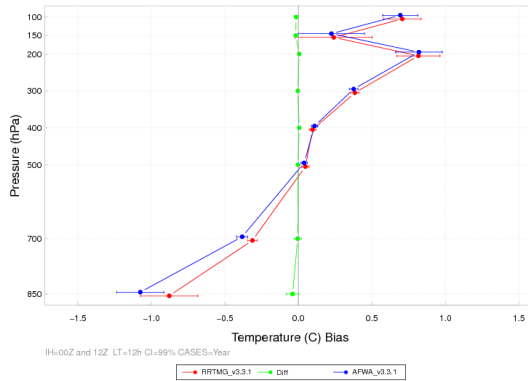
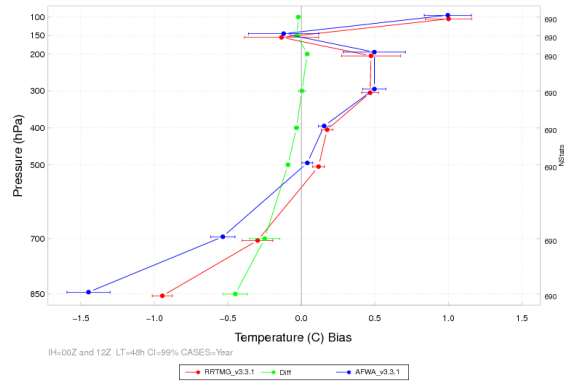


Figure 4. Vertical profile of the median BCRMSE for temperature (°C) for the full integration domain aggregated across the entire year of cases for the (a) 12- and (b) 48-h lead times. The AFWA configuration is in blue, the RRTMG configuration in red, and the pair-wise differences (AFWA-RRTMG) in green. The horizontal bars attached to the median represent the 99% CIs.

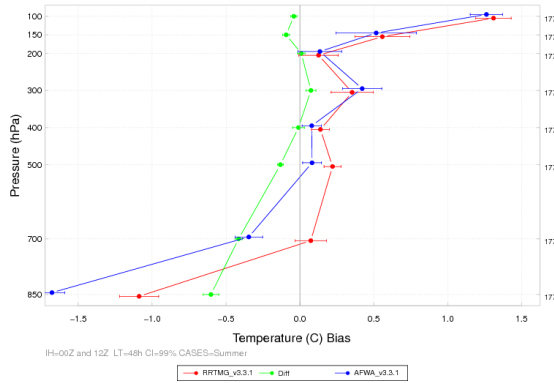
(a) Annual LT=12 h



(b) Annual LT=48 h



(c) Summer LT=48 h



(d) Winter LT=48 h

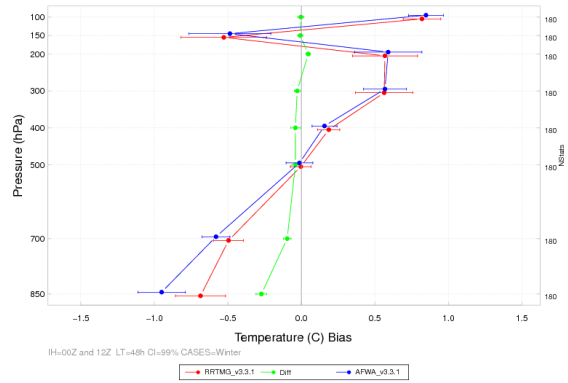
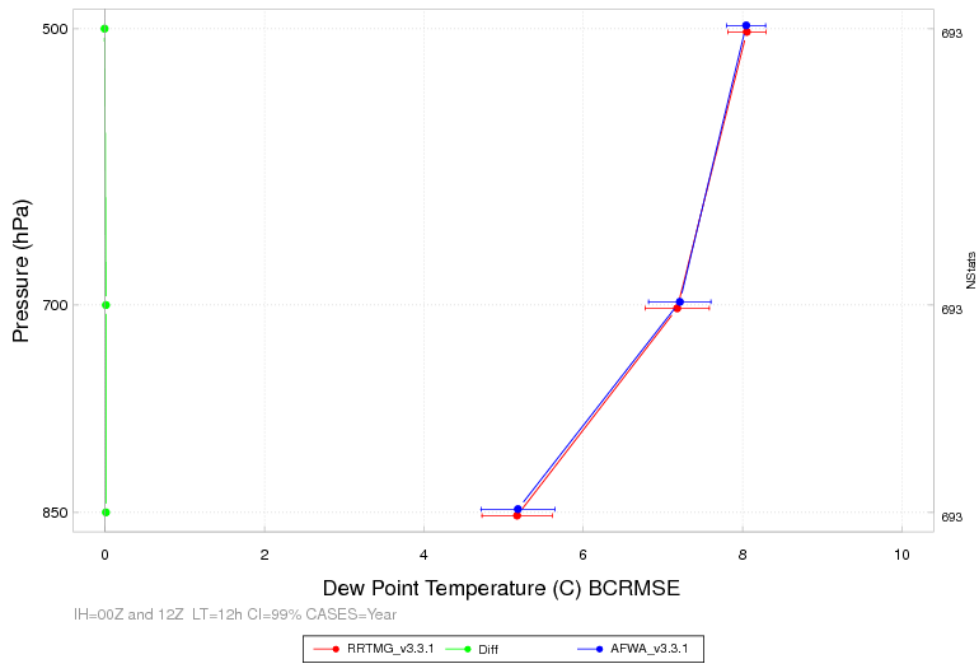


Figure 5. Vertical profile of the median bias for temperature ($^{\circ}\text{C}$) for the full integration domain aggregated across the entire year of cases for the (a) 12- and (b) 48-h lead times and for 48-h lead time for the (c) summer aggregation and (d) winter aggregation. The AFWA configuration is in blue, the RRTMG configuration in red, and the pair-wise differences (AFWA-RRTMG) in green. The horizontal bars attached to the median represent the 99% CIs.

(a) LT=12 h



(b) LT=48 h

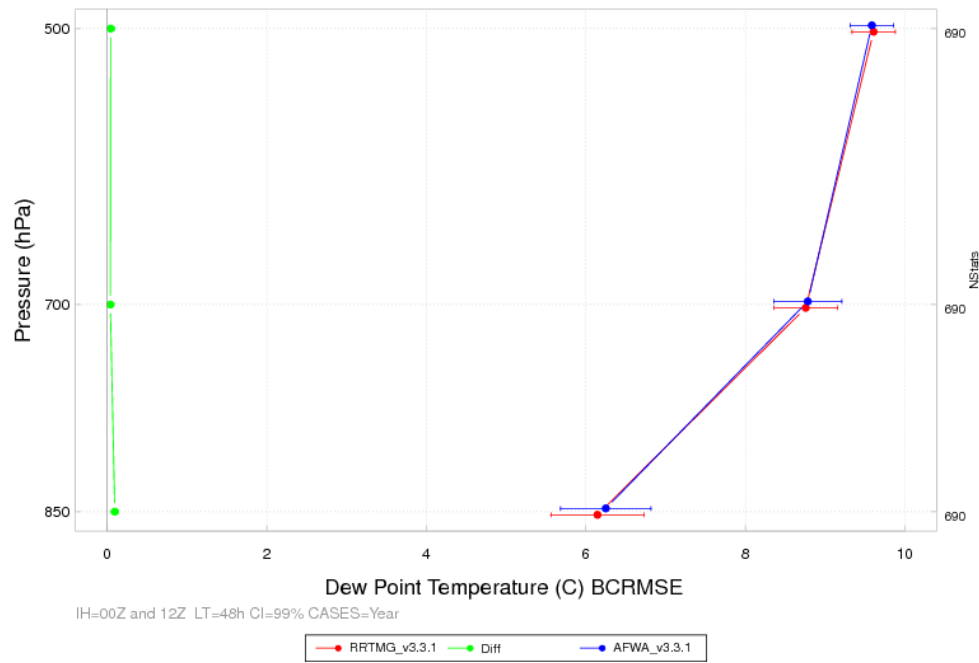
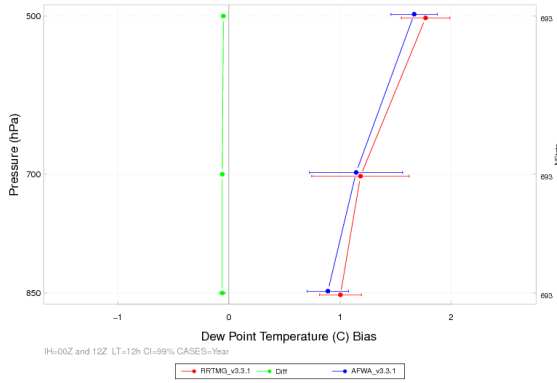
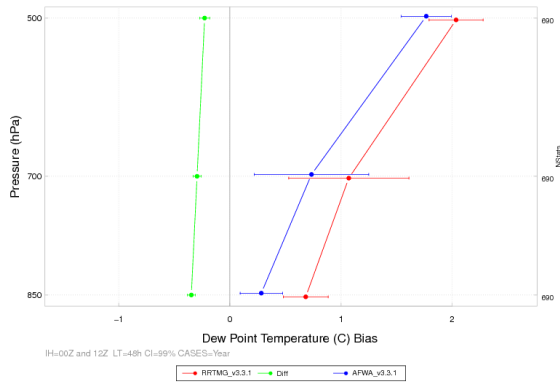


Figure 6. Vertical profile of the median BCRMSE for dew point temperature ($^{\circ}\text{C}$) for the full integration domain aggregated across the entire year of cases for the (a) 12- and (b) 48-h lead times. The AFWA configuration is in blue, the RRTMG configuration in red, and the pair-wise differences (AFWA-RRTMG) in green. The horizontal bars attached to the median represent the 99% CIs.

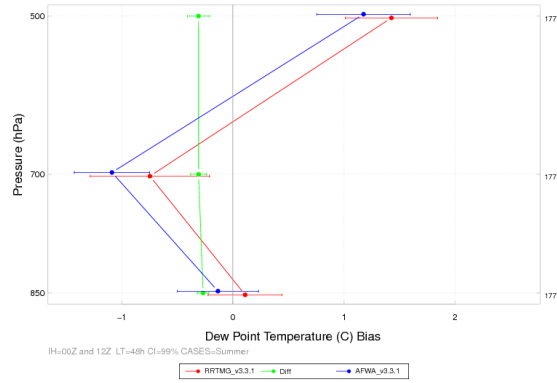
(a) Annual LT=12 h



(b) Annual LT=48 h



(c) Summer LT=48 h



(d) Winter LT=48 h

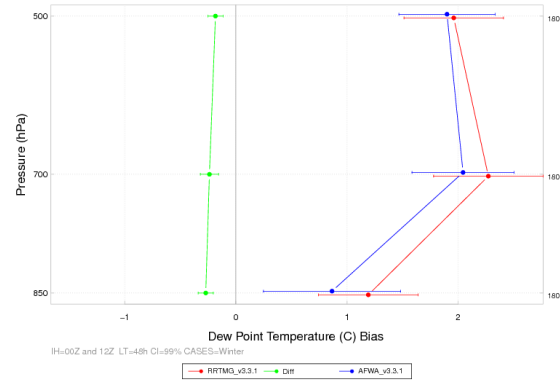
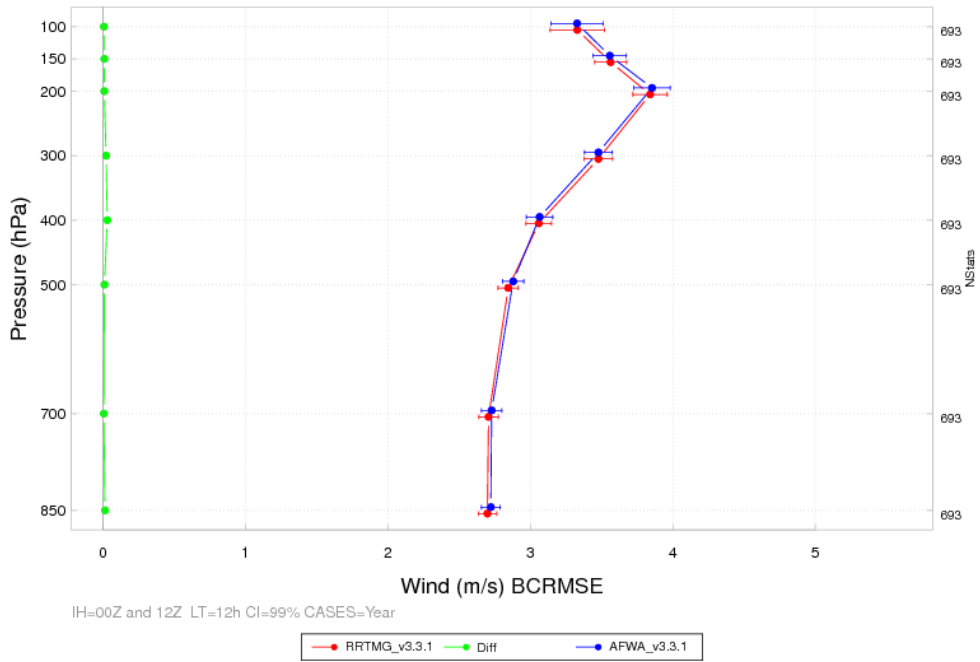


Figure 7. Vertical profile of the median bias for dew point temperature ($^{\circ}\text{C}$) for the full integration domain aggregated across the entire year of cases for the (a) 12- and (b) 48-h lead times and for 48-h lead time for the (c) summer aggregation and (d) winter aggregation. The AFWA configuration is in blue, the RRTMG configuration in red, and the pair-wise differences (AFWA-RRTMG) in green. The horizontal bars attached to the median represent the 99% CIs.

(a) LT=12 h



(b) LT=48 h

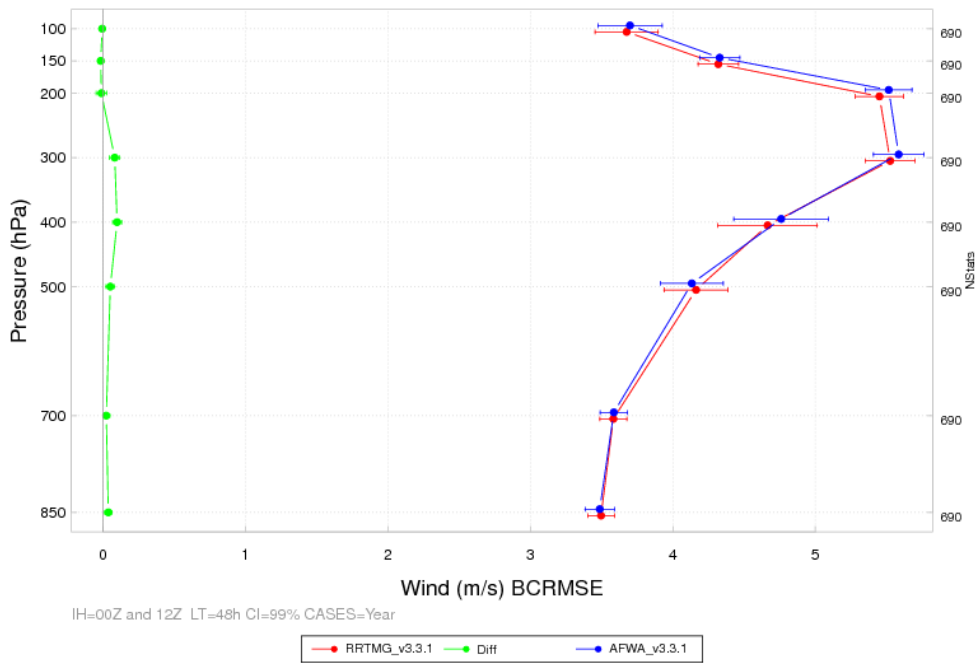
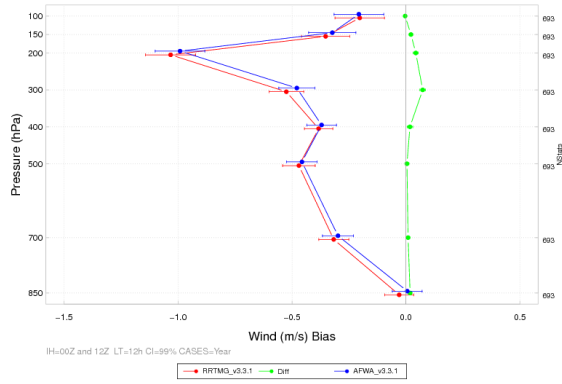
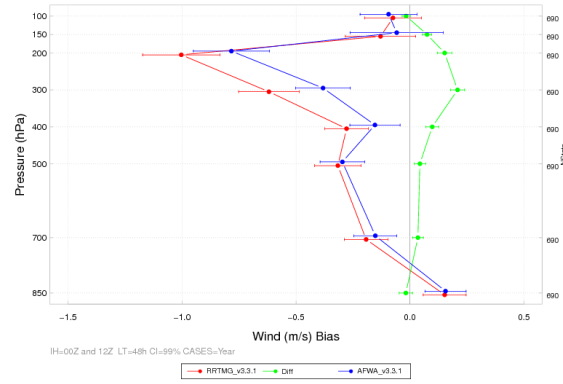


Figure 8. Vertical profile of the median BCRMSE for wind speed (m s^{-1}) for the full integration domain aggregated across the entire year of cases for the (a) 12- and (b) 48-h lead times. The AFWA configuration is in blue, the RRTMG configuration in red, and the pair-wise differences (AFWA-RRTMG) in green. The horizontal bars attached to the median represent the 99% CIs.

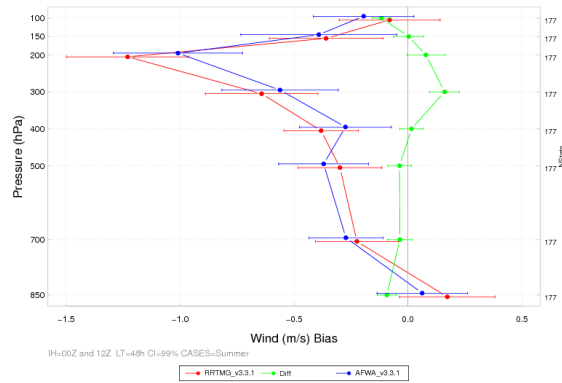
(a) Annual LT=12 h



(b) Annual LT=48 h



(c) Summer LT=48 h



(d) Winter LT=48 h

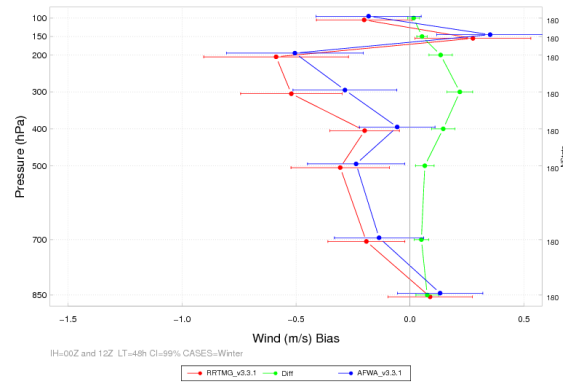
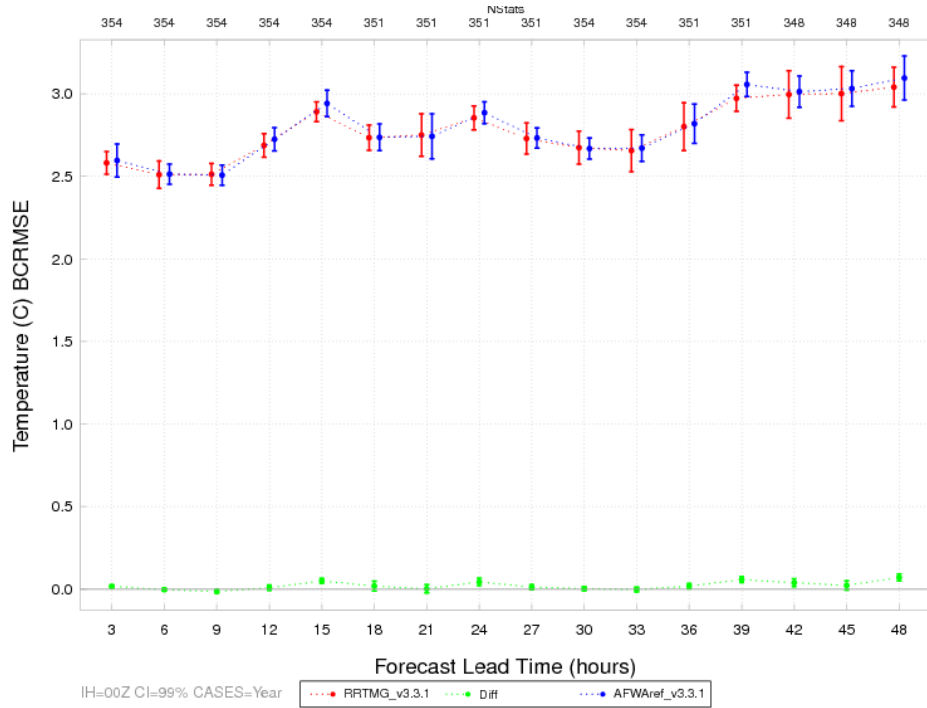


Figure 9. Vertical profile of the median bias for wind speed (m s^{-1}) for the full integration domain aggregated across the entire year of cases for the (a) 12- and (b) 48-h lead times and for 48-h lead time for the (c) summer aggregation and (d) winter aggregation. The AFWA configuration is in blue, the RRTMG configuration in red, and the pair-wise differences (AFWA-RRTMG) in green. The horizontal bars attached to the median represent the 99% CIs.

(a) IH=00 UTC



(b) IH=12 UTC

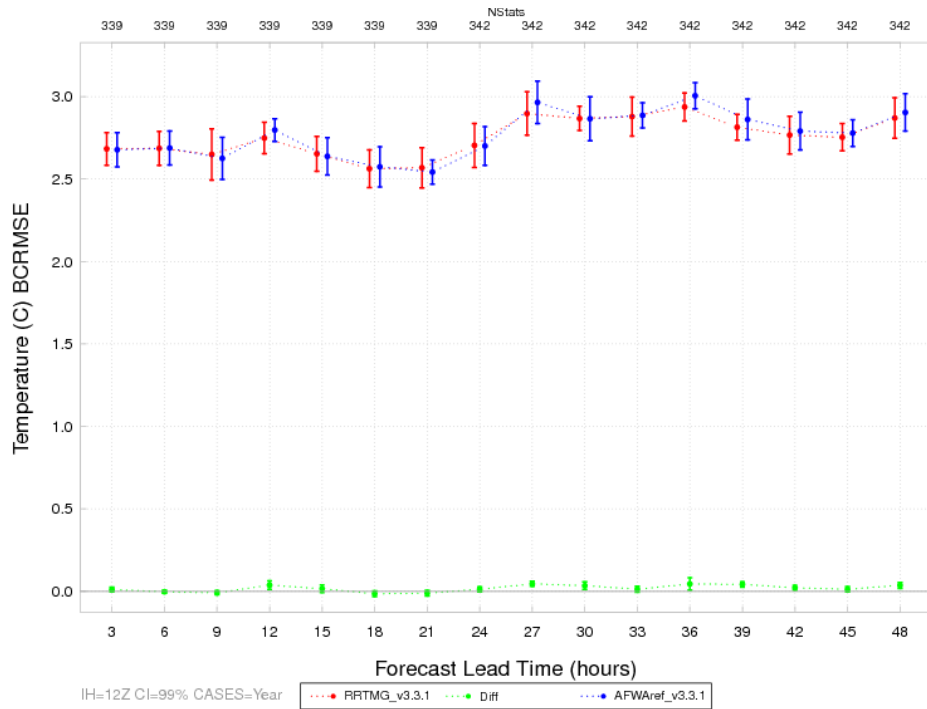
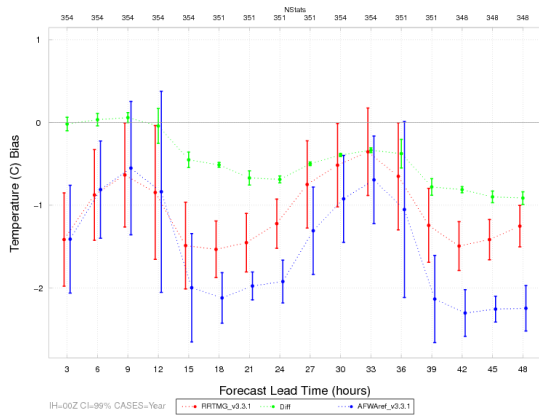
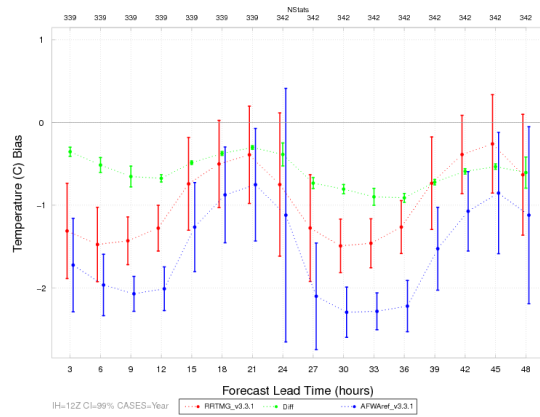


Figure 10. Time series plot of 2 m AGL temperature ($^{\circ}\text{C}$) for median BCRMSE for the (a) 00 UTC initializations and (b) 12 UTC initializations aggregated across the entire year of cases. The AFWA configuration is in blue, the RRTMG configuration in red, and the pair-wise differences (AFWA-RRTMG) in green. The vertical bars attached to the median represent the 99% CIs.

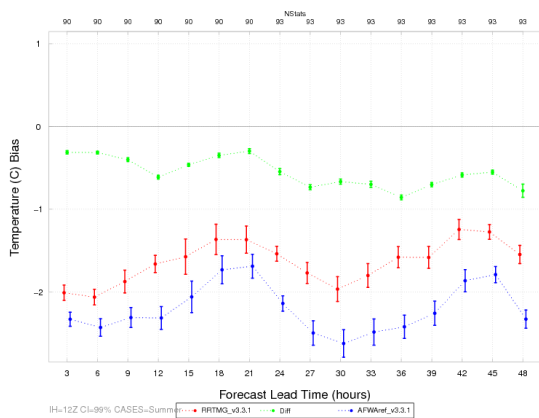
(a) Annual IH=00 UTC



(b) Annual IH=12 UTC



(c) Summer IH=12 UTC



(d) Winter IH=12 UTC

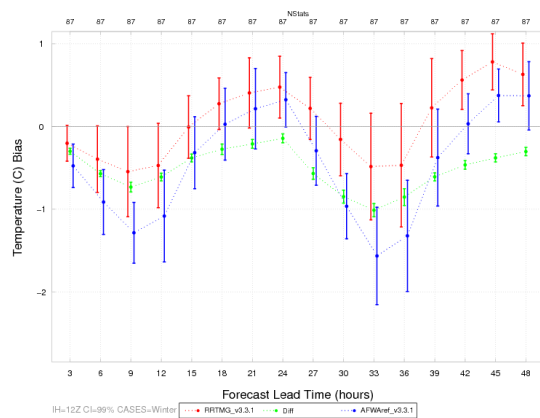
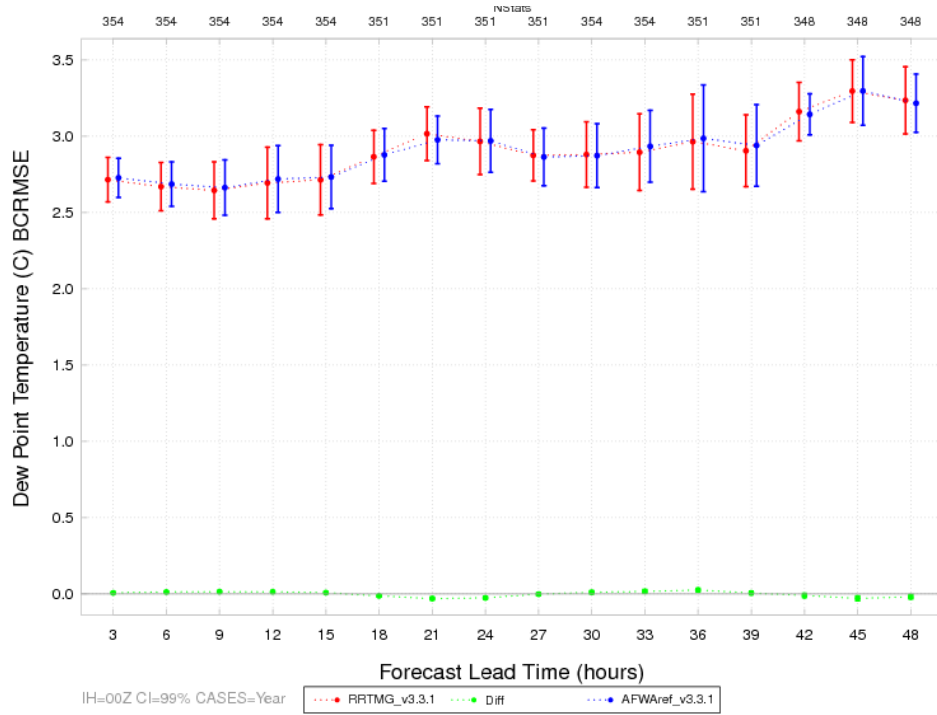


Figure 11. Time series plot of 2 m AGL temperature ($^{\circ}\text{C}$) for median bias for the full integration domain aggregated across the entire year of cases for the (a) 00 UTC initializations and (b) 12 UTC initializations and for the (c) summer aggregation and (d) winter aggregation. The AFWA configuration is in blue, the RRTMG configuration in red, and the differences (AFWA-RRTMG) in green. The vertical bars attached to the median represent the 99% CIs.

(a) IH=00 UTC



(b) IH=12 UTC

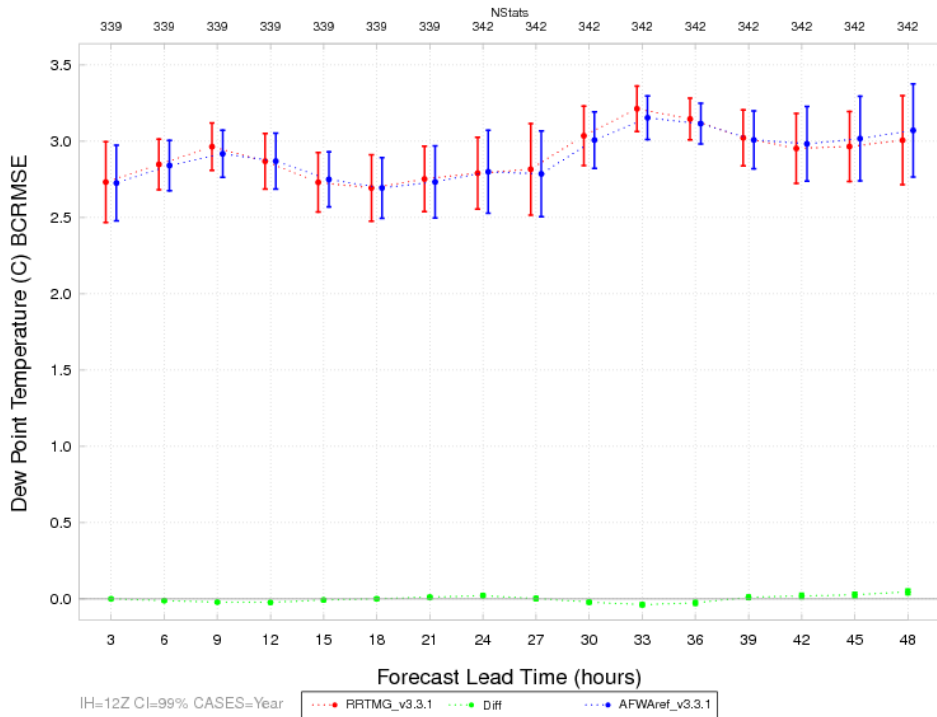
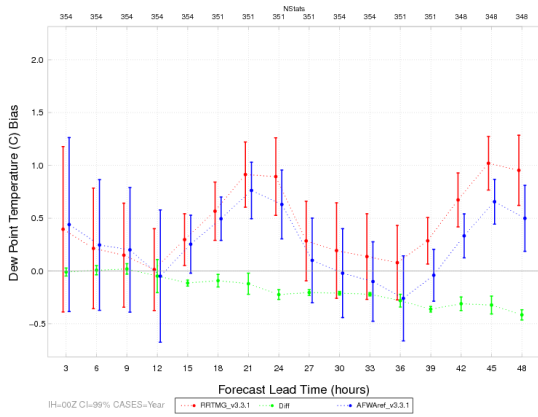
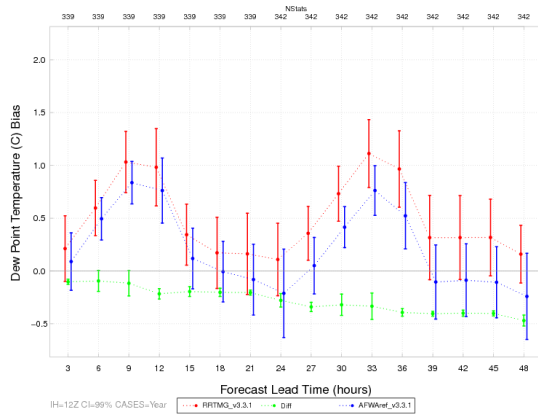


Figure 12. Time series plot of 2 m AGL dew point temperature (°C) for median BCRMSE for the (a) 00 UTC initializations and (b) 12 UTC initializations aggregated across the entire year of cases. The AFWA configuration is in blue, the RRTMG configuration in red, and the pair-wise differences (AFWA-RRTMG) in green. The vertical bars attached to the median represent the 99% CIs.

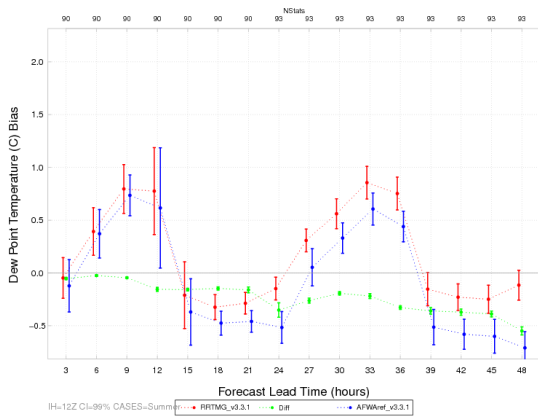
(a) Annual IH=00 UTC



(b) Annual IH=12 UTC



(c) Summer IH=12 UTC



(d) Winter IH=12 UTC

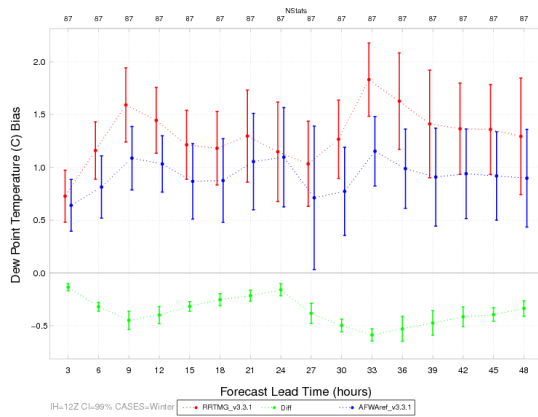
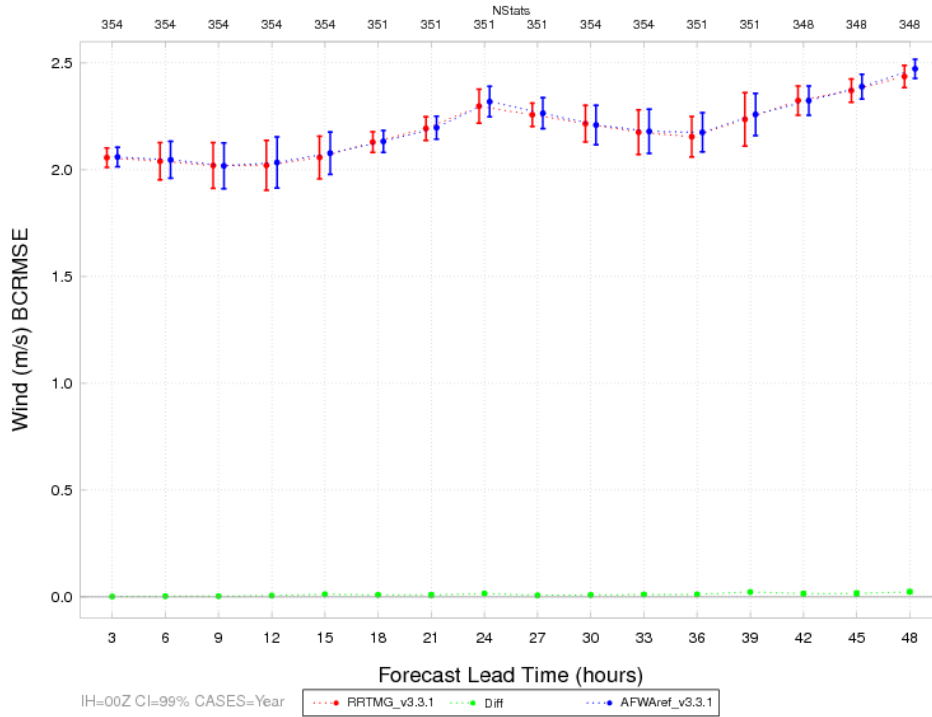


Figure 13. Time series plot of 2 m AGL dew point temperature ($^{\circ}\text{C}$) for median bias for the full integration domain aggregated across the entire year of cases for the (a) 00 UTC initializations and (b) 12 UTC initializations and for the 12 UTC initializations for the (c) summer aggregation and (d) winter aggregation. The AFWA configuration is in blue, the RRTMG configuration in red, and the pair-wise differences (AFWA-RRTMG) in green. The vertical bars attached to the median represent the 99% CIs.

(a) IH=00 UTC



(b) IH=12 UTC

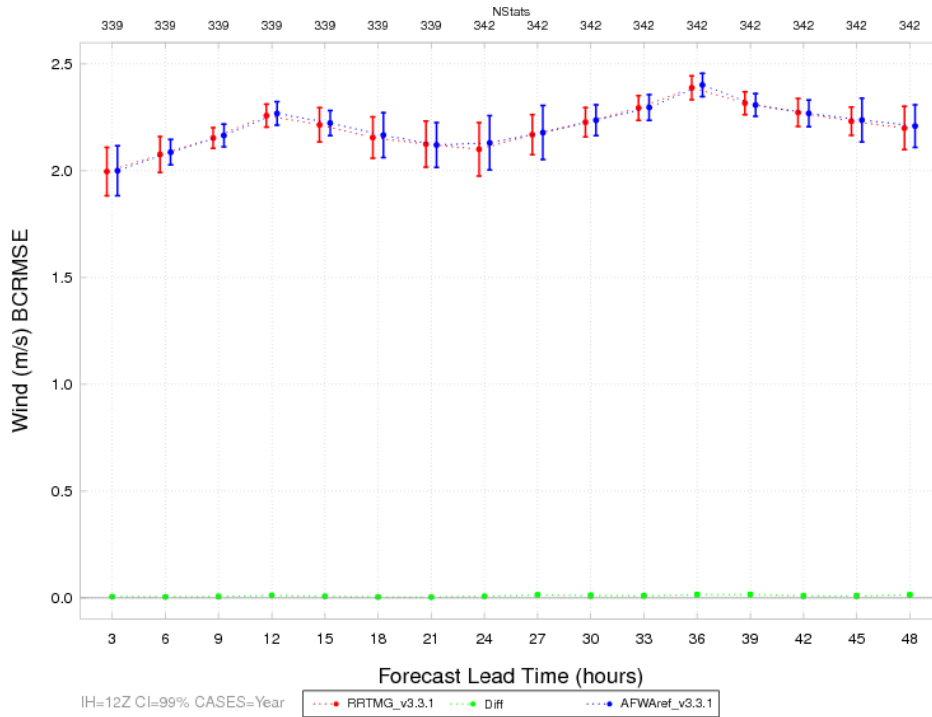
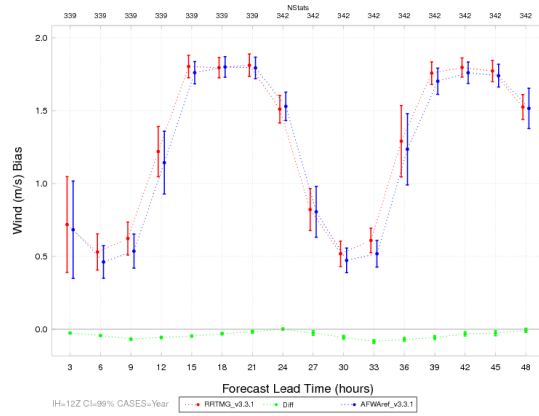


Figure 14. Time series plot of 10 m AGL wind speed (m s^{-1}) for median BCRMSE for the 12 UTC initializations (a) aggregated across the entire year of cases and (b) aggregated across the summer season. The AFWA configuration is in blue, the RRTMG configuration in red, and the pair-wise differences (AFWA-RRTMG) in green. The vertical bars attached to the median represent the 99% CIs.

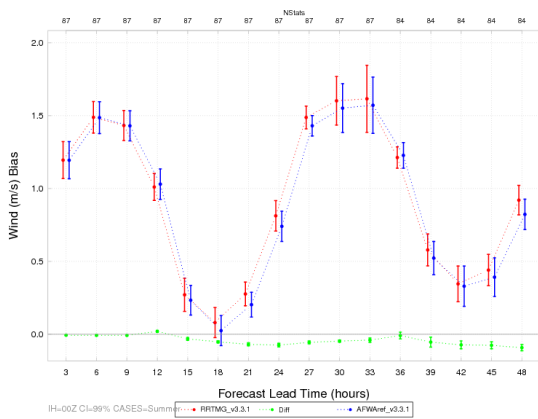
(a) Annual IH=00 UTC



(b) Annual IH=12 UTC



(c) Summer IH=00 UTC



(d) Winter IH=00 UTC

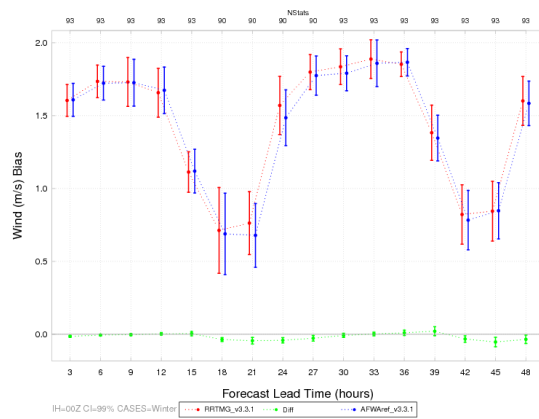
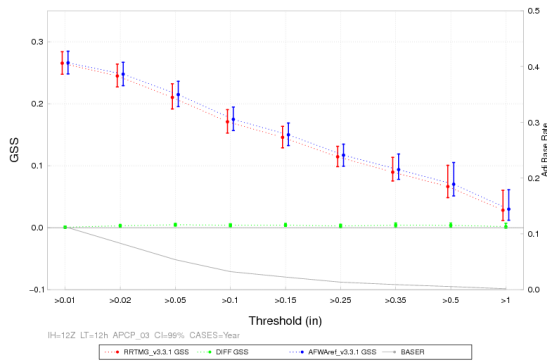
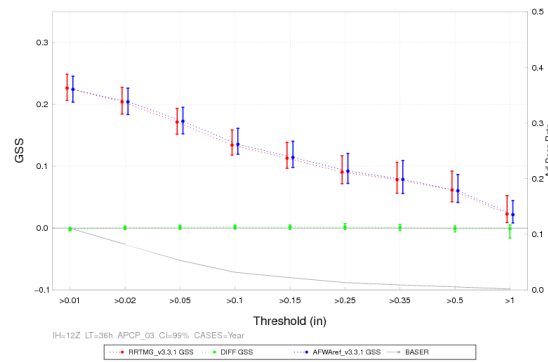


Figure 15. Time series plot of 2 m AGL wind speed (m s^{-1}) for median bias for the full integration domain aggregated across the entire year of cases for the (a) 00 UTC initializations and (b) 12 UTC initializations and for the 00 UTC initializations for the (c) summer aggregation and (d) winter aggregation. The AFWA configuration is in blue, the RRTMG configuration in red, and the differences (AFWA-RRTMG) in green. The vertical bars attached to the median represent the 99% CIs.

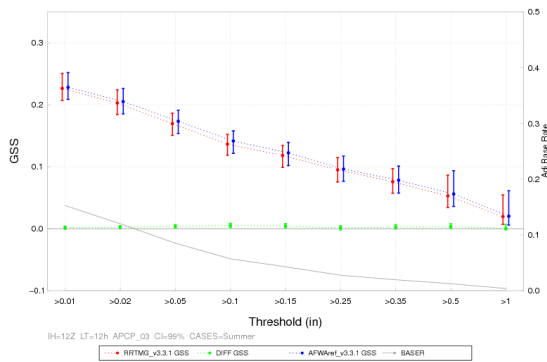
(a) Annual LT=12 h



(b) Annual LT=36 h



(c) Summer LT=12 h



(d) Winter LT=12 h

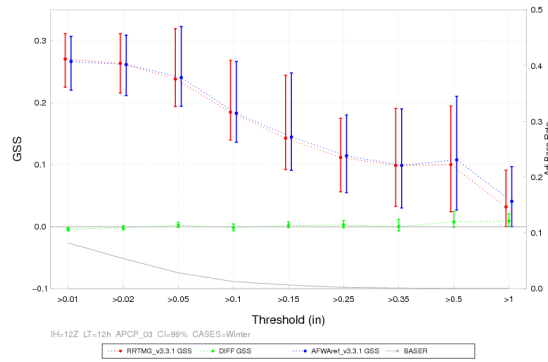
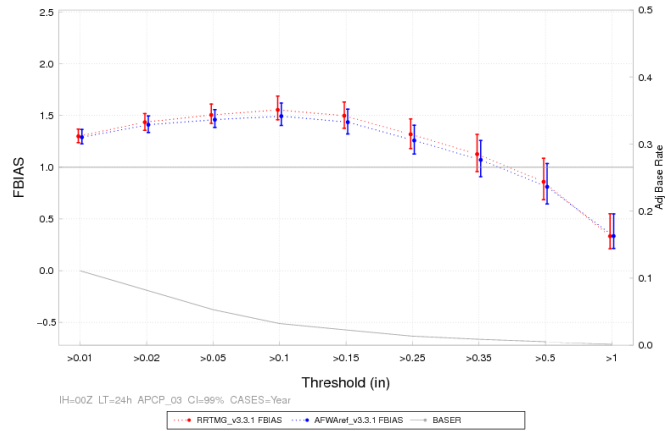
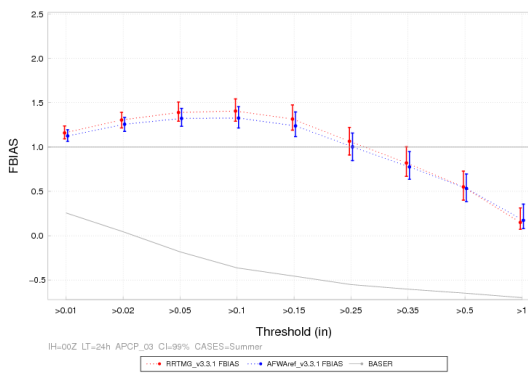


Figure 16. Threshold series plot of 3-h accumulated precipitation (in) for median GSS for the 12 UTC initializations aggregated across the entire year of cases for the (a) 12-h lead time and the (b) 36-h lead time and for the 12 UTC initializations for the 12-h lead time for the (c) summer aggregation and (d) winter aggregation. The AFWA configuration is in blue, the RRTMG configuration in red, and the pair-wise differences (AFWA-RRTMG) in green. The vertical bars attached to the median represent the 99% CIs.

(a) Annual



(b) Summer



(c) Winter

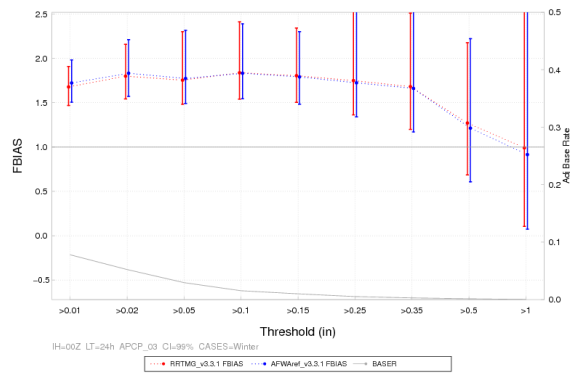
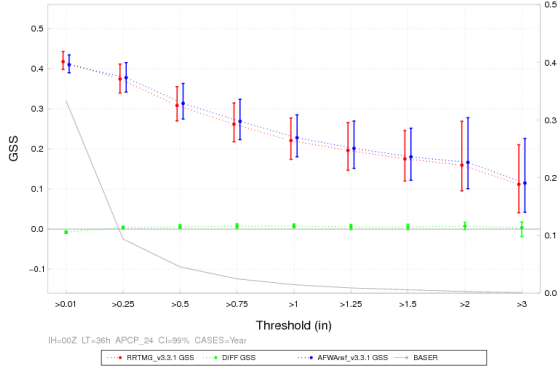
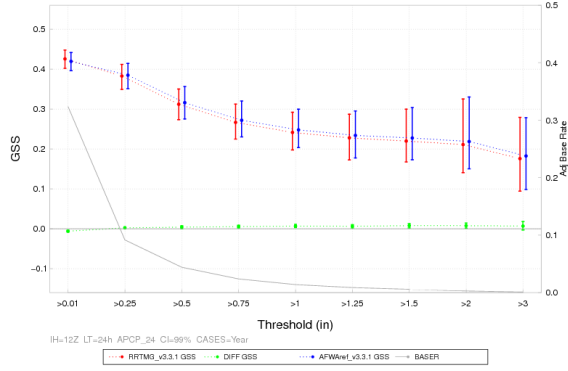


Figure 17. Threshold series plot of 3-h accumulated precipitation (in) for median frequency bias for the 00 UTC initialization for the 24-h lead time aggregated across the (a) entire year of cases, (b) summer aggregation, and (c) winter aggregation. The AFWA configuration is in blue, the RRTMG configuration in red, and the differences (AFWA-RRTMG) in green. The vertical bars attached to the median represent the 99% CIs.

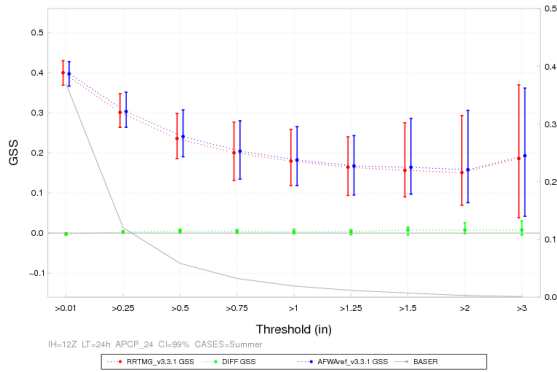
(a) Annual IH=00 UTC LT=36 h



(b) Annual IH=12 UTC LT=24 h



(c) Summer IH=12 UTC LT=24 h



(d) Winter IH=12 UTC LT=24 h

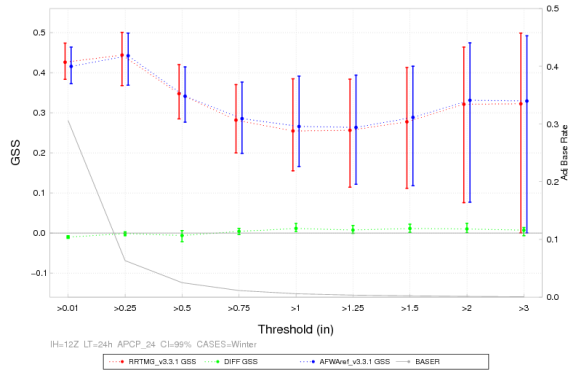
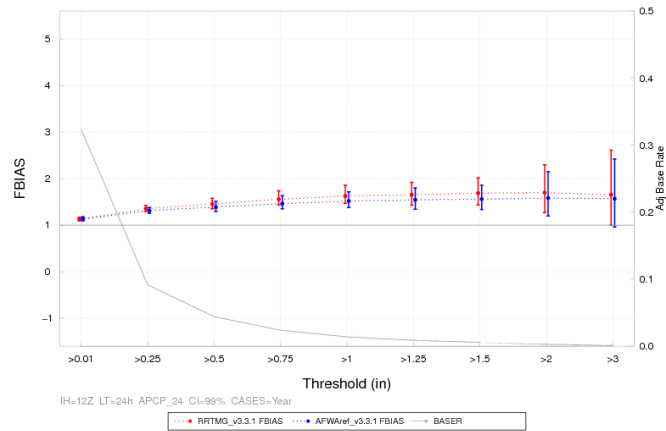
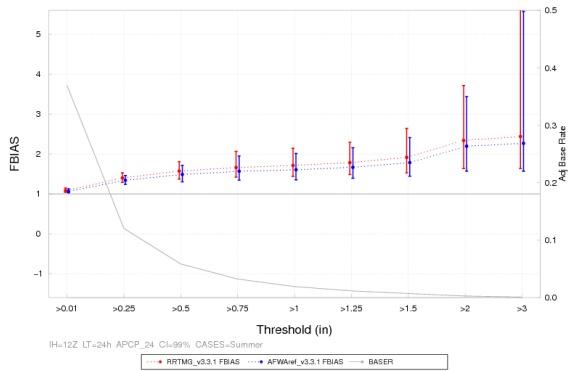


Figure 18. Threshold series plot of 24-h accumulated precipitation (in) for median GSS for the (a) 00 UTC for the 36-h lead time aggregated across the entire year of cases, the 12 UTC initialization for the 24-h lead time aggregated across the (b) entire year of cases, (c) summer aggregation, and (d) winter aggregation. The AFWA configuration is in blue, the RRTMG configuration in red, and the differences (AFWA-RRTMG) in green. The vertical bars attached to the median represent the 99% CIs.

(a) Annual



(b) Summer



(c) Winter

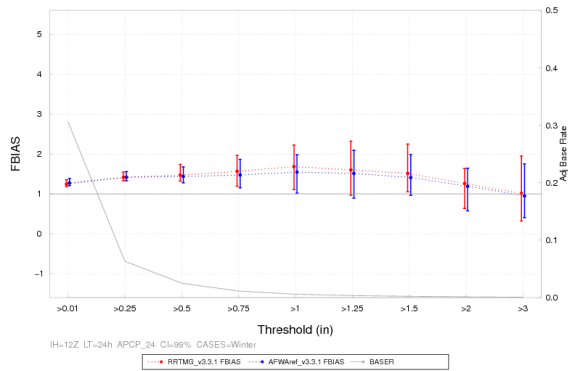


Figure 19. Threshold series plot of 24-h accumulated precipitation (in) for median frequency bias for the 12 UTC initializations for the 24-h lead time aggregated across the (a) entire year of cases, (b) summer aggregation, and (c) winter aggregation. The AFWA configuration is in blue, the RRTMG configuration in red, and the differences (AFWA-RRTMG) in green. The vertical bars attached to the median represent the 99% CIs.

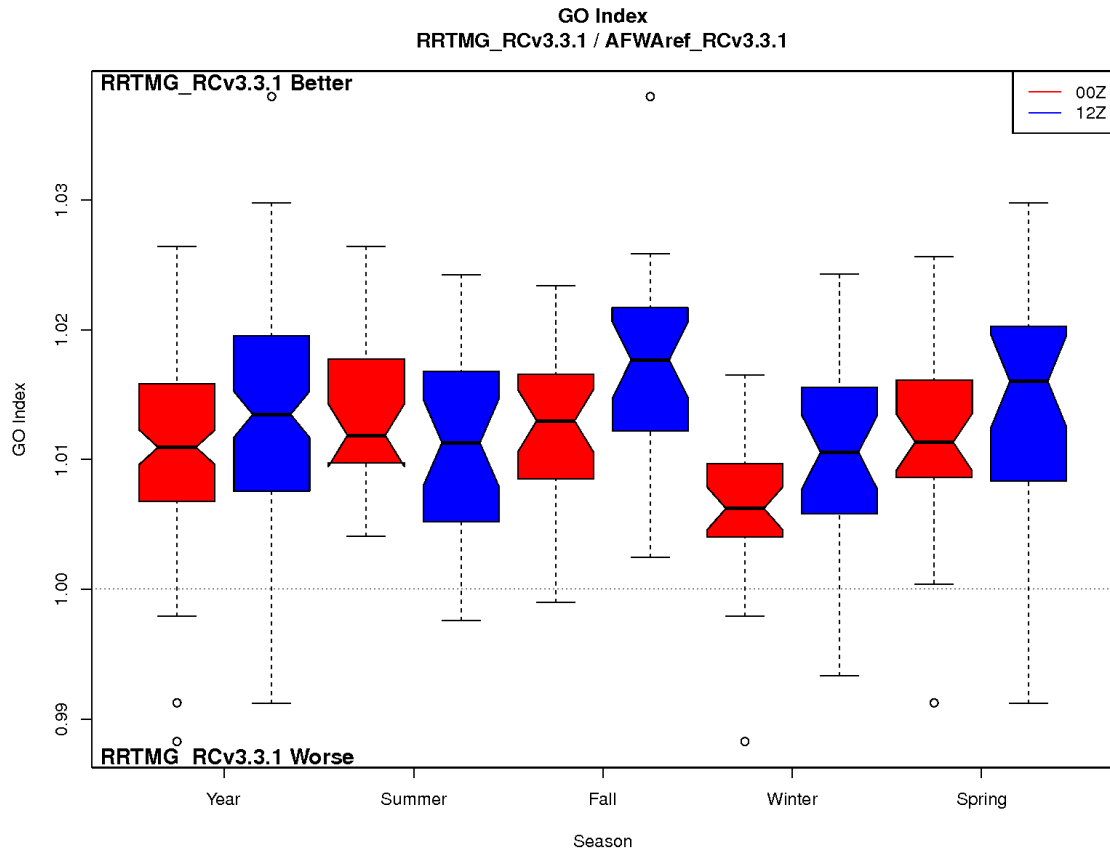


Figure 20. Boxplot of GO Index values aggregated across the entire year of cases and for all seasons, stratified by initialization time where 00 UTC is in red and 12 UTC is in blue. The median value is the thick black line located at the vertex of the notches, the notches around the median is an approximation of the 95% confidence about the median, the whiskers, denoted by the black, dashed lines, denote the largest values that are not outliers, and the circles represent the outliers.

Appendix A: Case list. Dates in bold were not included in the verification due to bad or missing input data.

00 UTC Initialization	12 UTC Initialization
June 2008: 4, 7, 10, 13, 16, 19, 22, 25, 28	June 2008: 2, 5, 8, 11, 14, 17, 20, 23, 26, 29
July 2008: 1, 4, 7, 10 , 13, 16, 19, 22, 25, 28, 31	July 2008: 2, 5, 8, 11, 14, 17, 20, 23, 26, 29
Aug 2008: 3, 6, 9, 12, 15, 18, 21, 24, 27, 30	Aug 2008: 1, 4, 7, 10, 13, 16, 19, 22, 25, 28, 31
Sept 2008: 2, 5, 8, 11, 14, 17, 20, 23, 26, 29	Sept 2008: 3, 6, 9, 12, 15 , 18, 21, 24, 27, 30
Oct 2008: 2, 5, 8, 11, 14, 17 , 20, 23, 26, 29	Oct 2008: 3, 6, 9, 12, 15 , 18 , 21 , 24, 27, 30
Nov 2008: 1, 4, 7, 10, 13, 16, 19, 22, 25, 28	Nov 2008: 2, 5, 8, 11, 14, 17, 20, 23, 26, 29
Dec 2008: 1, 4, 7, 10, 13, 16, 19, 22, 25, 28, 31	Dec 2008: 2, 5, 8, 11 , 14, 17, 20, 23, 26, 29
Jan 2009: 3, 6, 9, 12, 15, 18, 21, 24, 27, 30	Jan 2009: 1, 4, 7, 10, 13, 16, 19, 22, 25, 28, 31
Feb 2009: 2, 5, 8, 11, 14, 17, 20, 23, 26	Feb 2009: 3, 6, 9, 12, 15, 18, 21, 24, 27
Mar 2009: 1, 4, 7, 10, 13, 16, 19, 22, 25, 28, 31	Mar 2009: 2, 5, 8, 11, 14, 17, 20, 23, 26, 29
April 2009: 3, 6, 9, 12, 15, 18, 21, 24, 27, 30	April 2009: 1 , 4, 7, 10, 13, 16, 19, 22 , 25, 28
May 2009: 3, 6, 9, 12, 15, 18, 21, 24 , 27, 30	May 2009: 1, 4, 7, 10, 13, 16, 19, 22, 25 , 28, 31

Appendix B: Subset a WRF *namelist.input* used in this test

```

&time_control
run_hours           = 48,
interval_seconds    = 10800,
history_interval    = 180,
frames_per_outfile  = 1,
restart             = .false.,
io_form_history     = 2,
/
&domains            = 90,
time_step_fract_num = 0,
time_step_fract_den = 1,
max_dom            = 1,
e_we              = 403,
e_sn              = 302,
e_vert            = 57,
num_metgrid_levels = 27,
dx                = 15000,
dy                = 15000,
p_top_requested    = 1000,
interp_type        = 1,
lowest_lev_from_sfc = .false.,
lagrange_order     = 1,
force_sfc_in_vinterp = 6,
zap_close_levels   = 500,
adjust_heights     = .true.,
eta_levels          = 1.000, 0.997, 0.992, 0.985, 0.978, 0.969, 0.960, 0.950,
                    0.938, 0.925, 0.910, 0.894, 0.876, 0.857, 0.835, 0.812,

```

0.787, 0.760, 0.731, 0.700, 0.668, 0.635, 0.600, 0.565,
0.530, 0.494, 0.458, 0.423, 0.388, 0.355, 0.323, 0.293,
0.264, 0.237, 0.212, 0.188, 0.167, 0.147, 0.130, 0.114,
0.099, 0.086, 0.074, 0.064, 0.054, 0.046, 0.039, 0.032,
0.027, 0.022, 0.017, 0.013, 0.010, 0.007, 0.004, 0.002,
0.000,

/

```
&physics
mp_physics           = 4,
ra_lw_physics        = 1,
ra_sw_physics        = 1,
radt                 = 30,
sf_sfclay_physics   = 1,
sf_surface_physics   = 2,
bl_pbl_physics       = 1,
bldt                 = 0,
cu_physics           = 1,
cudt                 = 5,
surface_input_source = 1,
num_soil_layers      = 4,
mp_zero_out          = 2,
/
&dynamics
rk_ord               = 3,
diff_6th_opt         = 2,
diff_6th_factor      = 0.10,
w_damping            = 1,
diff_opt             = 1,
km_opt               = 4,
damp_opt             = 0,
base_temp            = 290.,
zdamp                = 5000.,
dampcoef             = 0.01,
khdif                = 0,
kvdif                = 0,
smdiv                = 0.1,
emdiv                = 0.01,
epssm                = 0.1,
non_hydrostatic      = .true.,
time_step_sound      = 0,
h_mom_adv_order      = 5,
v_mom_adv_order      = 3,
h_sca_adv_order      = 5,
v_sca_adv_order      = 3,
moist_adv_opt        = 1,
scalar_adv_opt        = 0,
chem_adv_opt          = 0,
tke_adv_opt          = 0,
/
&bdy_control
spec_bdy_width       = 5,
spec_zone             = 1,
relax_zone           = 4,
specified             = .true.,
/
```